

JCU ScholarShip

Morphing Triangle Contact Representations of Triangulations

Item Type	Article
Authors	Angelini, Patrizio;Chaplick, Steven;Cornelsen, Sabine;Da Lozzo, Giordano;Roselli, Vincenzo
Citation	Angelini, Patrizio, Steven Chaplick, Sabine Cornelsen, Giordano Da Lozzo, and Vincenzo Roselli. "Morphing Triangle Contact Representations of Triangulations." <i>Discrete & Computational Geometry</i> 70 (3): 991–1024. 2023.
DOI	https://doi.org/10.1007/s00454-022-00475-9
Publisher	Springer Nature
Rights	Attribution 4.0 International
Download date	2026-03-06 05:48:31
Item License	http://creativecommons.org/licenses/by/4.0/
Link to Item	https://hdl.handle.net/20.500.14490/328



Morphing Triangle Contact Representations of Triangulations

Patrizio Angelini¹ · Steven Chaplick² · Sabine Cornelsen³ ·
Giordano Da Lozzo⁴ · Vincenzo Roselli⁴

Received: 27 July 2021 / Revised: 29 March 2022 / Accepted: 14 May 2022 /

Published online: 15 March 2023

© The Author(s) 2023

Abstract

A *morph* is a continuous transformation between two representations of a graph. We consider the problem of morphing between contact representations of a plane graph. In an \mathcal{F} -*contact representation* of a plane graph G , vertices are realized by internally disjoint elements from a family \mathcal{F} of connected geometric objects. Two such elements touch if and only if their corresponding vertices are adjacent. These touchings also induce the same embedding as in G . In a morph between two \mathcal{F} -contact representations we insist that at each time step (continuously throughout the morph) we have an \mathcal{F} -contact representation. We focus on the case when \mathcal{F} is the family of triangles in \mathbb{R}^2 that are the lower-right half of axis-parallel rectangles. Such *RT-representations* exist for every plane graph and right triangles are one of the simplest families of shapes supporting this property. Moreover, they naturally correspond to 3-orientations. Thus, they provide a natural case to study regarding morphs of contact representations of plane graphs. We characterize the pairs of RT-representations admitting a morph between each other via the respective 3-orientations. Our characterization leads to a polynomial-time algorithm to decide whether there is a morph between two RT-representations of an n -vertex plane triangulation, and, if so, computes a morph with $\mathcal{O}(n^2)$ steps. Each of these steps is a *linear morph* moving the endpoints of each triangle at constant speed along straight-line trajectories. Our characterization also implies that for 4-connected plane triangulations there is a morph between every pair of RT-representations where the “top-most” triangle in both representations corresponds to the same vertex.

Editor in Charge: Csaba D. Tóth

This research began at the Graph and Network Visualization Workshop 2018 (GNV'18) in Heiligkreuztal. Our work was supported in part by the German Research Foundation DFG grant WO 758/11-1 (Chaplick), by DFG - Project-ID 50974019 - TRR 161 (B06) (Cornelsen), by MIUR Project “AHeAD” under PRIN 20174LF3T8, and by H2020-MSCA-RISE project 734922 - “CONNECT” (Da Lozzo and Roselli).

Extended author information available on the last page of the article

Keywords Planar graphs · Graph drawing · Morphing · Contact representation

Mathematics Subject Classification 05C10 · 05C85

1 Introduction

We consider the morphing problem from the perspective of geometric representations of graphs. While a lot of work has been done to understand how to planarly morph the standard node-link diagrams and to “rigidly” morph¹ configurations of geometric objects, comparatively little has been explicitly done regarding (non-rigid) morphing of alternative representations of planar graphs, e.g., contact systems of geometric objects such as disks or triangles. In this case, the planarity constraint translates into the requirement of continuously maintaining a representation of the appropriate type throughout the morph.

More formally, let \mathcal{F} be a family of geometric objects homeomorphic to a disk. An \mathcal{F} -contact representation of a plane graph G maps vertices to internally disjoint elements of \mathcal{F} , where we assume that a *plane graph* has a fixed set of faces and a fixed outer face (see, e.g., Fig. 1). We denote the geometric object representing a vertex v by $\Delta(v)$. Objects $\Delta(v)$ and $\Delta(w)$ touch if and only if $\{v, w\}$ is an edge. The contact system of the objects must induce the same faces and outer face as in G . A *morph* between two \mathcal{F} -contact representations R_0 and R_1 of a plane graph G is a continuously changing family of \mathcal{F} -contact representations R_t of G indexed by time $t \in [0, 1]$ which means in particular that the boundary points of the geometric objects move along continuous trajectories from their starting to their ending position. An implication of the existence of morphs between any two representations of the same type is that the topological space defined by such representations is connected. We are interested in elementary morphs, and in particular in *linear morphs*, where the boundary points of the geometric objects move at constant speed along straight-line trajectories from their starting to their ending position. A *piecewise linear morph of length ℓ* between two \mathcal{F} -contact representations R_0 and R_ℓ of a plane graph G is a sequence $\langle R_0, \dots, R_\ell \rangle$ of \mathcal{F} -contact representations of G such that there is a linear morph between R_i and R_{i+1} for $i = 0, \dots, \ell - 1$. For a background on the mathematical aspects of morphing, see, e.g., [3].

1.1 Morphs of Node-Link Diagrams

A *node-link diagram* is a drawing of a graph in the plane where each vertex is represented as a point and each edge as a Jordan arc connecting its end vertices. In a *plane node-link diagram* of a plane graph edges do not cross and both the set of faces and the outer face are maintained. Fáry’s theorem tells us that every plane graph has a plane node-link diagram where the edges are mapped to line segments. Of course, for a given plane graph G , there can be many such node-link diagrams of G , and the goal of the work in planar morphing is to study how (efficiently) one can create a smooth

¹ Scaling the objects is not allowed, e.g., as in *bar-joint* systems [45] or in *body-hinge* systems [16, 23, 26].

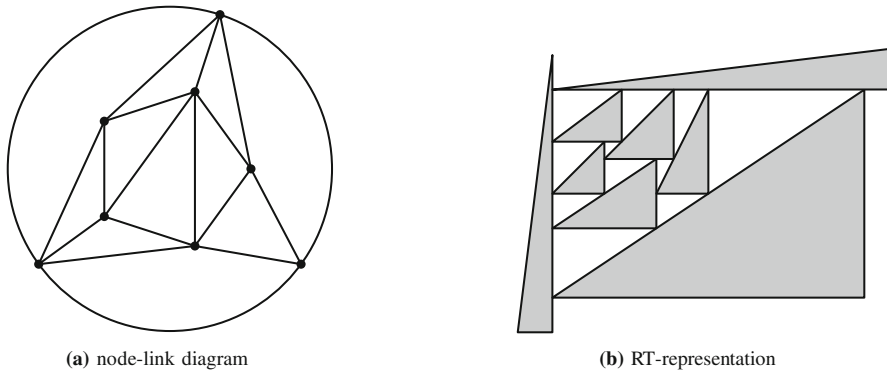


Fig. 1 Two representations of the same plane graph G . **a** A node-link diagram of G and **b** a contact representation of G using right-angle triangles, i.e., an RT-representation

(animated) transition from one such node-link diagram to another while maintaining planarity. Already in the 1940's Cairns [19] proved that, for plane triangulations, planar morphs exist between any pair of plane node-link diagrams. However, the construction involved exponentially-many morphing steps. Floater and Gotsman [33], and Gotsman and Surazhsky [39, 50] gave a different approach via Tutte's graph drawing algorithm [53], but this involves non-linear trajectories of unbounded complexity. Thomassen [51] and Aronov et al. [11] independently showed that two plane node-link diagrams of the same plane graph have a *compatible triangulation*² thereby lifting Cairns' result to plane graphs. Of particular interest is the study of *linear morphs*, where each vertex moves at a uniform speed along a straight-line. After several intermediate results to improve the complexity of the morphs [2, 7] and to remove the necessity of computing compatible triangulations [9], an algorithm to construct a planar morph between any pair of plane node-link diagrams of any n -vertex plane graph using $\Theta(n)$ linear steps was presented [1]. Such a morph can be computed in $\mathcal{O}(n^2 \log n)$ time [41]. For triconnected planar graphs, a different approach to obtain a linear number of linear morphs was recently presented by Erickson and Lin [28].

Planar morphs of other specialized plane node-link diagrams have also been considered, e.g., planar orthogonal drawings [15, 36, 37], convex drawings [8, 28, 40, 41], upward planar drawings [25], small-area drawings of trees [13], and so-called *Schnyder drawings* [14]. In this latter result the lattice structure of all Schnyder woods of a plane triangulation [17, 29] is exploited in order to obtain a sequence of linear morphs within a grid of quadratic size. Finally, planar morphs on the surface of the sphere [42] or the torus [20, 28] and in three dimensions have been investigated [12]. Beyond planarity, morphs have been recently considered for subclasses of 1-planar graphs [6].

² i.e., a way to triangulate both diagrams to produce the same plane triangulation.

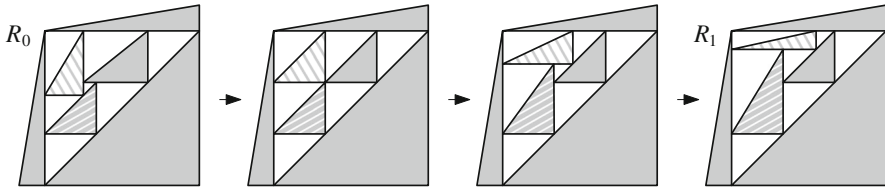


Fig. 2 An illustration of a morph between two RT-representations R_0 and R_1 of the same plane triangulation. All the intermediate representations between any two consecutive RT-representations above are obtained by interpolating the corners of each triangle along linear trajectories

1.2 Morphs of Contact Representations

Similar to Fáry’s theorem, the well-known Koebe–Andreev–Thurston theorem [4, 44] states that every plane graph G has a *coin* representation, i.e., an \mathcal{F} -contact representation where \mathcal{F} is the set of all disks. Additionally, for the case of triangulated plane graphs, such coin representations of G are unique up to *Möbius transformations* [18]—see [31] for a modern treatment. There has been a lot of work on how to intuitively understand and animate such transformations (see, e.g., the work of Arnold and Rogness [10]), i.e., for our context, how to morph between two coin representations. Of course, ambiguity remains regarding how to formalize the complexity of such morphs. In particular, this connection to Möbius transformations appears to indicate that a theory of piecewise linear morphing for coin representations would be quite limited.

For this reason, we instead focus on contact representations of convex polygons. These shapes still allow for representing all plane triangulations, as a direct consequence of the Koebe–Andreev–Thurston theorem, but are more amenable to piecewise linear morphs, where the linearity is defined on the trajectories of the corners; see, for example, the morph depicted in Fig. 2. De Fraysseix et al. [35] showed that every plane graph G has a contact representation by triangles, and observed that these triangle-contact representations correspond to the 3-orientations (i.e., the *Schnyder woods*) of G . Schrenzenmaier [49] used Schnyder woods to show that each 4-connected triangulation has a contact representation with homothetic triangles. Gonçalves et al. [38] extended the triangle-contact results from triangulations [35] to 3-connected plane graphs, by showing that Felsner’s generalized Schnyder woods [29] correspond to *primal-dual* triangle-contact representations. Note that triangles and coins are not the only families of shapes that have been studied from the perspective of contact representations. Some further examples include boxes in \mathbb{R}^3 [22, 30, 52], line segments [34, 43], and homothetic polygons [24, 32, 48]. Recently, the problem of morphing restricted contact representations of axis-parallel rectangles, more precisely so called *rectangular duals*, has been considered [21].

The construction of triangle-contact representations [35] (and the correspondence to 3-orientations) can be adjusted so that each triangle is the lower-right half of an axis-parallel rectangle. These *right-triangle representations* (RT-representations) are our focus; see Fig. 1.

1.3 Our Contribution and Outline

We characterize the pairs of RT-representations of the same plane graph G that admit a morph. This characterization is based on the relationship between (degenerate) RT-representations and the Schnyder woods of G , and involves the existence of a special path in the distributive lattice of the Schnyder woods of G . More precisely, we prove that a morph between two RT-representations exists if and only if the corresponding Schnyder woods can be obtained from each other by reversing oriented inner faces of the triangulation only. The characterization leads to an efficient decision algorithm to test for the existence of a morph. Furthermore, in the positive case, the algorithm constructs a piecewise linear morph of quadratic length. This implies that, although elementary, piecewise linear morphs are as “powerful” as general morphs.

The paper is organized as follows. We start with some definitions in Sect. 2 and describe the relationship between (degenerate) RT-representations and Schnyder woods of plane triangulations in Sect. 3. In particular, we show that any morph between two RT-representations can be associated with a special sequence of Schnyder woods (Theorem 3.4). In Sect. 4, we provide sufficient geometric conditions for a linear morph between two RT-representations. The first condition is that each corner c of a triangle touches the same side s of another triangle in the two representations. By the described relationship, this corresponds to the fact that the morph happens within the same Schnyder wood. The second condition ensures that the contact between c and s is maintained. This is fulfilled if s has the same slope in the two RT-representations or if the point of s hosting c is defined by the same convex combination of the end-points of s in both representations. In Sect. 5, we present our morphing algorithm. If the two input RT-representations correspond to different Schnyder woods, we consider a path (if any) between them in the lattice structure of all Schnyder woods, similar to [14], that satisfies the necessary properties stated in Theorem 3.4. When moving along this path, from a Schnyder wood to another, we construct intermediate RT-representations that simultaneously correspond to both woods. We provide an algorithm to construct such intermediate RT-representations that results in a linear morph at each step. Finally, in Sect. 6, we show how to decide whether there exists a path in the lattice structure that satisfies the required properties. This results in an efficient testing algorithm for the existence of a piecewise linear morph between two RT-representations of a plane triangulation; in the positive case, the computed piecewise linear morph has at most quadratic length. Consequently, for 4-connected plane triangulations, under a natural condition on the outer face of their RT-representations, the topological space defined by such RT-representations is connected.

2 Definitions and Preliminaries

2.1 Basics

Throughout this paper we consider simple graphs without loops and parallel edges. A *plane triangulation* is a maximal planar graph with a distinguished outer face. A *directed acyclic graph (DAG)* is an oriented graph with no directed cycles. A *topologi-*



Fig. 3 The two conditions for a Schnyder wood

cal ordering of an n -vertex DAG $G = (V, E)$ is a one-to-one map $\tau : V \rightarrow \{1, \dots, n\}$ such that $\tau(v) < \tau(w)$ for $(v, w) \in E$. Let p and q be two points in the plane. The line segment \overline{pq} is the set $\{(1 - \lambda)p + \lambda q : 0 \leq \lambda \leq 1\}$ of convex combinations of p and q . Considering \overline{pq} oriented from p to q , we say that x cuts \overline{pq} with the ratio λ if $x = (1 - \lambda)p + \lambda q$.

In the case of polygons, a linear morph is completely specified by the initial and final positions of the corners of each polygon. If a corner p is at position p_0 in the initial representation (at time $t = 0$) and at position p_1 in the final representation (at time $t = 1$), then its position at time t during a linear morph is $(1 - t)p_0 + tp_1$ for any $0 \leq t \leq 1$.

2.2 Schnyder Woods

A 3-orientation [17, 29] of a plane triangulation is an orientation of the inner edges such that each inner vertex has out-degree 3 and the three outer vertices have out-degree 0. A Schnyder wood T [47] of a plane triangulation G is a 3-orientation together with a partition of the inner edges into three color classes, such that the three outgoing edges of an inner vertex have distinct colors and all the incoming edges of an outer vertex have the same color. Moreover, the color assignment around the vertices must be as indicated in Fig. 3: The clockwise ordering of the colors of the three outgoing edges is the same for each inner vertex (say red, green, blue) and all incoming edges of a certain color are between the two outgoing edges of the other two colors (e.g. the red incoming edges, if any, are between the blue and the green outgoing edge). We say that a cycle in a Schnyder wood is oriented if it is a directed cycle.

The following well-known properties of Schnyder woods can directly be deduced from the work of Schnyder [47].

- (i) Every plane triangulation has a 3-orientation.
- (ii) For each 3-orientation of a plane triangulation there is exactly one partition of the inner edges into three color classes such that the pair yields a Schnyder wood.
- (iii) Each color class of a Schnyder wood induces a directed spanning tree rooted at an outer vertex.
- (iv) Reversing the edges of two color classes and maintaining the orientation of the third color class yields a directed acyclic graph.

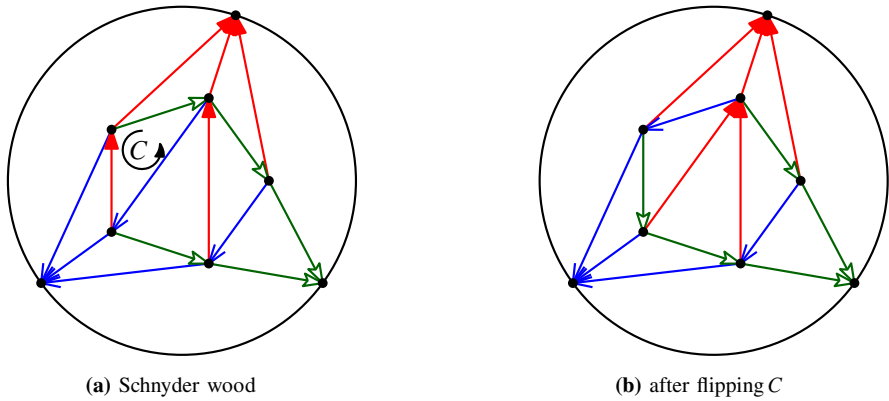


Fig. 4 A counter-clockwise flip of an oriented facial triangle C in a Schnyder wood

- (v) The edges of an oriented triangle in a Schnyder wood have three distinct colors and every triangle composed of edges of three different colors is oriented.

We call the color classes red (r, \blacktriangleright), blue (b, \blacktriangleright), and green (g, \blacktriangleright). The symbols X_r , X_b , and X_g denote the *red*, *blue*, and *green outer vertex* of G , i.e., the outer vertices with incoming red, blue, and green edges, respectively. For an inner vertex v , let v_r , v_b , and v_g be the respective neighbors of v such that (v, v_r) is red, (v, v_b) is blue, and (v, v_g) is green. Finally, let $DAG_r(T)$ ($DAG_b(T)$) be the directed acyclic graph obtained from G by orienting all red (blue) edges as in T while all blue (red) and green edges are reversed.

Let C be an oriented triangle of a Schnyder wood T . Reversing C yields another 3-orientation with its unique Schnyder wood T_C . If C is a *facial cycle*, i.e., the boundary of an internal face, then T differs from T_C by recoloring the edges on C only. See Fig. 4 for an example. More precisely, the new outgoing edge of a vertex gets the color of the former outgoing edge of the same vertex. This procedure of reversing and recoloring is called *flipping*³ an oriented triangle of a Schnyder wood. Any Schnyder wood can be converted into any other Schnyder wood of the same plane triangulation by flipping $\mathcal{O}(n^2)$ oriented triangles [14, 17]. For two Schnyder woods T_0 and T_ℓ , $\langle C_1, \dots, C_\ell \rangle$ is a *flip sequence between T_0 and T_ℓ* if there are Schnyder woods $T_1, \dots, T_{\ell-1}$ such that $C_i, i = 1, \dots, \ell$, is an oriented triangle in T_{i-1} and T_i is obtained from T_{i-1} by flipping C_i . We say that a *Schnyder wood T' can be obtained from a Schnyder wood T by a sequence of facial flips* if there is a flip sequence between T and T' that contains only facial cycles.

3 RT-Representations of Plane Triangulations

Let R be an RT-representation of a plane triangulation G and let u be a vertex of G . Recall that the triangle $\Delta(u)$ representing u is the lower-right half of an axis-parallel

³ Brehm [17] called *flip* and *flip* the operations of flipping a counter-clockwise triangle and a clockwise triangle, respectively.

rectangle. We use $\triangleleft(u)$, $\triangleup(u)$, and $\nearrow(u)$ to denote the *horizontal*, *vertical*, and *diagonal* side of $\Delta(u)$. The *topmost* vertex of R is the vertex v of G for which the y -coordinate of $\triangleleft(v)$ is maximum. Further, we let $\ulcorner(u)$, $\lrcorner(u)$, and $\top(u)$ denote the left, right, and top corner of $\Delta(u)$, respectively. If two triangles touch each other in their corners, we say that these two corners *coincide*. We call a face $f = \langle u, v, w \rangle$ *degenerate* if $\top(u)$, $\ulcorner(v)$, $\lrcorner(w)$ pairwise coincide (in which case f corresponds to a single point), see Fig. 5(b). An RT-representation is *degenerate* if it contains a degenerate face; otherwise, it is *non-degenerate*. Let (c, s) be a pair with $c \in \{\ulcorner, \lrcorner, \top\}$ and $s \in \{\triangleleft, \triangleup, \nearrow\}$, we say that (c, s) is a *compatible pair* if it belongs to the set $\{(\lrcorner, \nearrow), (\ulcorner, \triangleup), (\top, \triangleleft)\}$. Observe that, if a corner c of a triangle $\Delta(u)$ touches the interior of a side s of a triangle $\Delta(v)$, with $(u, v) \in E(G)$, then (c, s) is a compatible pair. On the other hand, when two corners coincide, there exist four different pairs composed of a corner and a side, two of which are compatible. E.g., if $\lrcorner(v)$ coincides with $\ulcorner(u)$ for two vertices u and v , then the two compatible pairs are (\ulcorner, \triangleup) and (\lrcorner, \nearrow) —even though $\lrcorner(v)$ also touches $\triangleleft(u)$ and $\ulcorner(u)$ touches $\triangleleft(v)$.

In the next two subsections, we describe the relationship between RT-representations and Schnyder woods [35] and extend it to the case of degenerate RT-representations. Along the way we will establish a condition on the existence of a morph between RT-representations and prove its necessity (Theorem 3.4).

3.1 From RT-Representations to Schnyder Woods

Let $G = (V, E)$ be a plane triangulation with a given RT-representation R . It is possible to orient and color the edges of G in order to obtain a Schnyder wood by considering the types of contacts between triangles in R as follows.

First, consider the non-degenerate case; refer to Fig. 5(a). Let $e = \{u, v\} \in E$ be an inner edge such that a corner c of $\Delta(u)$ touches a side s of $\Delta(v)$. We use the following rules: We orient e from u to v , and color e *blue* if c is $\ulcorner(u)$, *green* if c is $\lrcorner(u)$, *red* if c is $\top(u)$. Observe that due to this convention the topmost vertex is X_r .

Lemma 3.1 [35, Thm. 2.2] *The above assignment yields a Schnyder wood.*

Assume now that there exist two triangles $\Delta(u)$ and $\Delta(v)$ whose corners coincide. Observe that the assignment of colors and directions to the edge $\{u, v\}$ determined by the procedure above would be ambiguous. The next observation will be useful to resolve this ambiguity.

Observation 3.2 *Consider an RT-representation of a plane triangulation and an edge $\{u, v\}$ that is not on the outer face. If a corner of the triangle $\Delta(u)$ coincides with a corner of the triangle $\Delta(v)$ in a point p , then $\{u, v\}$ is incident to a degenerate face.*

Proof Let f_ℓ and f_r be the two triangular faces to the left and the right of $\{u, v\}$, and let w_ℓ and w_r be the vertex incident to f_ℓ and f_r , respectively, that is different from u and v . Then, $\Delta(w_\ell)$ and $\Delta(w_r)$ must both touch $\Delta(u)$ and $\Delta(v)$, and they must be on different sides of p , unless one of f_ℓ and f_r is the outer face. This implies that either $\Delta(w_\ell)$ or $\Delta(w_r)$ has a corner on p .

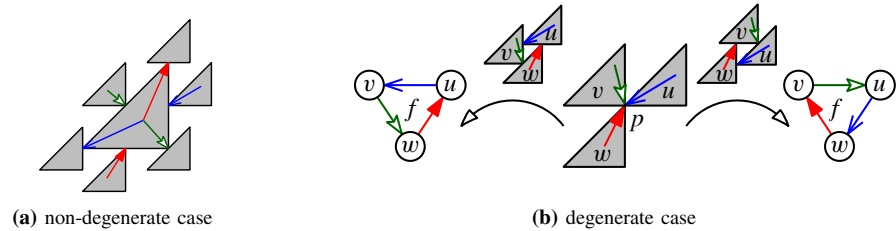


Fig. 5 From an RT-representation to a Schnyder wood

An immediate consequence of Observation 3.2 is that whenever three triangles intersect in a common point then they bound a degenerate face. Consider now a degenerate face f . For each of the three edges bounding f , a choice of coloring and orientation corresponds to deciding which of the two triangles participates to the touching with its corner and which triangle with an extremal point of one of its sides, which in turn corresponds to choosing one of the two compatible pairs determined by the touching. This yields two options as indicated in Fig. 5(b), both resulting in a Schnyder wood. Note that the face f is cyclic in both these Schnyder woods, and each of them can be obtained from the other by flipping f .

Summarizing, we get the following.

Observation 3.3 *Given an RT-representation R of a plane triangulation G , let P be the set of points where three triangles intersect. Then, R corresponds to a set \mathcal{T}_R of $2^{|P|}$ different Schnyder woods on G , the points of P correspond to $|P|$ edge-disjoint oriented faces, and the Schnyder woods in \mathcal{T}_R differ in flipping some of them.*

Observe that there is always a planar morph between two RT-representations of a graph with three vertices. See Fig. 10. This is in general no longer true for triangulations with separating triangles.

Theorem 3.4 (necessary condition) *If there is a (not necessarily piecewise linear) morph between two RT-representations of a plane triangulation G with more than three vertices, then the corresponding Schnyder woods can be obtained from each other by a sequence of facial flips. In particular the topmost vertex is the same in both representations.*

Proof Let $R_t, t \in [0, 1]$, be a morph between two RT-representations R_0 and R_1 of G . Consider moments in time t_1, \dots, t_k defined as follows. Let $t_1 = 0$ and $t_k = 1$. Given $t_i < 1$, let t_{i+1} be maximum such that $\mathcal{T}_{R_{t_i}} \cap \mathcal{T}_{R_{t_{i+1}}} \neq \emptyset$, where \mathcal{T}_R is the set of Schnyder woods corresponding to an RT-representation R as defined in Observation 3.3. Such a $t_{i+1} > t_i$ exists: First of all, observe that there exists a Schnyder wood $T \in \mathcal{T}_{R_{t_i}}$ that also occurs at a later moment t , i.e., such that $T \in \mathcal{T}_{R_t}$ for some $t > t_i$. More precisely, since morphs are continuous there is always an $\epsilon > t_i$ such that $\mathcal{T}_{R_{t_i}} \cap \mathcal{T}_{R_\epsilon} \neq \emptyset$. Second, we show that such a maximum moment in time exists. Let $T \in \mathcal{T}_{R_{t_i}}$. The moments in time in which T occurs form closed intervals. The maxima of these intervals form an increasing sequence in a compact subset of the reals and, thus, converge to the supremum t_T . Due to continuity there must exist an $\epsilon > 0$ such that $\mathcal{T}_{R_{t_i}} \subseteq \mathcal{T}_{R_{t_T}}$

for $t_T - \epsilon \leq t \leq t_T$. Since t_T is the supremum of moments in time in which the Schnyder wood T occurs it follows that $T \in \mathcal{T}_{R_{t_T}}$. Since $|\mathcal{T}_{R_{t_i}}|$ is finite, it follows that $t_{i+1} = \max_{T \in \mathcal{T}_{R_{t_i}}} t_T$.

Now let $T_i \in \mathcal{T}_{R_{t_i}} \cap \mathcal{T}_{R_{t_{i+1}}}$, $i = 1, \dots, k - 1$. Then T_{i+1} and T_i are both contained in $\mathcal{T}_{R_{t_{i+1}}}$. Thus, by Observation 3.3, T_{i+1} can be obtained from T_i by a sequence of edge-disjoint facial flips. Hence, any Schnyder wood of R_1 can be obtained from any Schnyder wood of R_0 by a sequence of facial flips.

The red outer vertex X_r cannot be changed by facial flips. Thus, the topmost vertex remains the same throughout the morph. Intuitively, changing the topmost vertex would require collapsing the outer 3-cycle into a single point. □

We will show that the necessary condition is also sufficient (Sect. 5), and can be tested in quadratic time (Sect. 6).

3.2 From Schnyder Woods to RT-Representations

Assume now that we are given a Schnyder wood T of a plane triangulation $G = (V, E)$. We describe a technique for constructing an RT-representation of G corresponding to T in which the y-coordinate of the horizontal side of each triangle is prescribed by a function $\tau : V \rightarrow \mathbb{R}$ satisfying some constraints. We would like to mention that in the non-degenerate case in [35], the function τ assigning the y-coordinates is a topological ordering of $\text{DAG}_r(T)$, also called a *canonical ordering* of G .

We call $\tau : V \rightarrow \mathbb{R}$ an *Admissible Degenerate Topological* labeling of the graph $\text{DAG}_r(T)$, for short *ADT-labeling*, if for each directed edge (u, v) of $\text{DAG}_r(T)$, we have

- (i) $\tau(u) \leq \tau(v)$ and
- (ii) $\tau(u) = \tau(v)$ only if (see Figs. 5(b) and 6(c)) the edge between u and v
 - is green and belongs to a clockwise oriented facial cycle, or
 - is blue and belongs to a counter-clockwise oriented facial cycle, and
- (iii) if $\tau(v_b) = \tau(v) = \tau(v_g)$ for a vertex v , and v_1 and v_2 are vertices such that $\langle v, v_g, v_1 \rangle$ is a clockwise facial cycle and $\langle v, v_b, v_2 \rangle$ is a counter-clockwise facial cycle, then $v_1 \neq v_2$ (see Fig. 7).

Lemma 3.5 *Let R be an RT-representation of a plane triangulation $G = (V, E)$, let T be a Schnyder wood corresponding to R , and let $\tau(v)$, $v \in V$, be the y-coordinate of $\triangleleft(v)$. Then, τ is an ADT-labeling of $\text{DAG}_r(T)$.*

Proof Let (u, v) be a directed edge of $\text{DAG}_r(T)$. By the definition of T , we get immediately that $\tau(u) \leq \tau(v)$ independently of whether (u, v) is red, green, or blue. In fact, if (u, v) is red, then it is oriented from u to v in T_r . Thus, the compatible pair corresponding to such an edge in R is $(\nearrow(u), \triangleleft(v))$. Hence, $\triangleleft(u)$ lies strictly below $\triangleleft(v)$. If (u, v) is green (resp., blue), then it is oriented from v to u in T . Thus, the compatible pair corresponding to such an edge in R is $(\triangleleft(v), \nearrow(u))$ (resp., $(\triangleleft(v), \nearrow(u))$). Hence, $\triangleleft(u)$ does not lie above $\triangleleft(v)$.

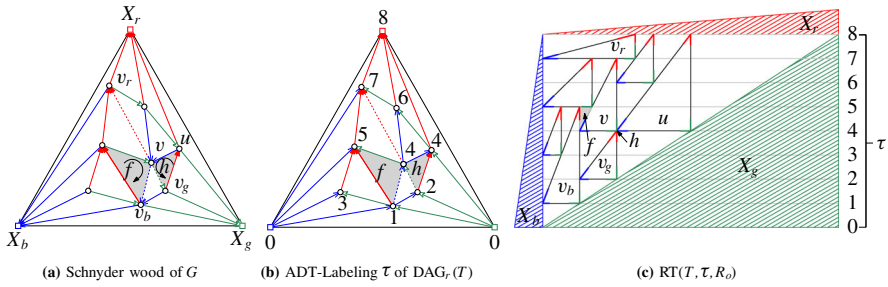


Fig. 6 (a) A Schnyder wood T of a plane triangulation G ; the edges connecting v with vertices $v_r, v_g,$ and v_b are dashed. (b) Graph $\text{DAG}_r(T)$ with ADT-labeling τ . (c) An RT-representation of G constructed from $T, \tau,$ and an RT-representation R_o of the outer face

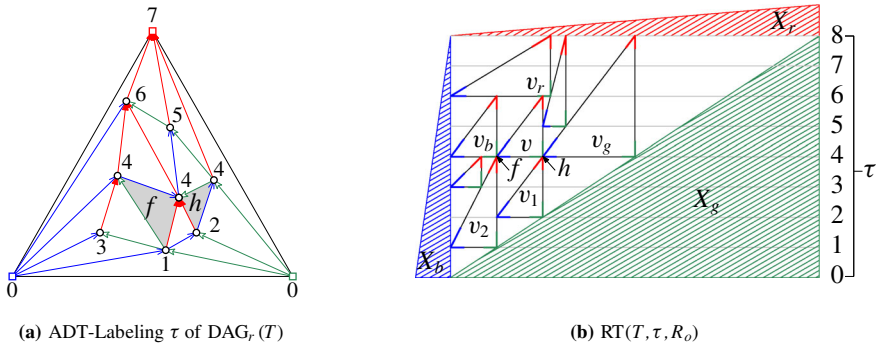


Fig. 7 Illustration of (iii) of an ADT-labeling where $\tau(v_b) = \tau(v) = \tau(v_g)$. Mind that, compared to Fig. 6, the faces f and h are flipped

Assume that $\tau(u) = \tau(v)$, which implies that (u, v) is not red, as observed above. Suppose that (v, u) is a green edge. Then, $\lrcorner(v)$ and $\llcorner(u)$ coincide. By Observation 3.2, there exists a vertex z such that $\lrcorner(z)$ coincides with $\lrcorner(v)$ and $\llcorner(u)$. Thus, $\langle v, u, z \rangle$ is a clockwise oriented facial cycle. Similarly, when (v, u) is a blue edge, there is a vertex z such that $\llcorner(v), \lrcorner(u)$, and $\lrcorner(z)$ coincide. Therefore, $\langle v, u, z \rangle$ is a counter-clockwise oriented facial cycle.

Finally, if $\tau(v_b) = \tau(v) = \tau(v_g)$ and v_1 and v_2 are the vertices such that $\langle v, v_g, v_1 \rangle$ is a clockwise facial cycle and $\langle v, v_b, v_2 \rangle$ is a counter-clockwise facial cycle, then $\lrcorner(v_1)$ touches $\lrcorner(v)$ and $\lrcorner(v_2)$ touches $\llcorner(v)$. See Fig. 7. Thus, $v_1 \neq v_2$. \square

Lemma 3.6 *Let T be a Schnyder wood of an n -vertex plane triangulation G , let τ be an ADT-labeling of $\text{DAG}_r(T)$, and let $R_o = \Delta(X_r) \cup \Delta(X_g) \cup \Delta(X_b)$ be an RT-representation of the outer face of G such that $\triangle(X_i)$ has y -coordinate $\tau(X_i)$, with $i \in \{r, g, b\}$. Then, there exists a unique RT-representation $\text{RT}(T, \tau, R_o)$ of G corresponding to T in which $\triangle(v)$ has y -coordinate $\tau(v)$, for each vertex v of G , and in which the outer face is drawn as in R_o .*

Proof Let $\tau': V \leftrightarrow \{1, 2, \dots, n\}$ be a topological ordering of $\text{DAG}_r(T)$. We process the vertices of G according to τ' . By the construction of $\text{DAG}_r(T)$, we have that

$\tau'(X_r) = n$ and either $\tau'(X_b) = 1$ and $\tau'(X_g) = 2$ or $\tau'(X_g) = 1$ and $\tau'(X_b) = 2$. Thus, in the first two steps and in the last step, we must draw triangles $\Delta(X_b)$, $\Delta(X_g)$, and $\Delta(X_r)$ as in R_o ; see Fig. 6(c).

At each of the intermediate steps, we consider a vertex v , with $\tau'(v) = i$, $2 < i < n$. Let R_{i-1} be the unique RT-representation of the subgraph G_{i-1} of G induced by the vertices preceding v in τ' under the conditions required in the lemma. Since the y -coordinates of the horizontal sides of the triangles are determined by τ and since $\nearrow(v)$ must touch $\triangleleft(v_r)$, we must draw $\Delta(v)$ so that its horizontal side has y -coordinate $\tau(v)$ and its top corner has y -coordinate $\tau(v_r)$. It remains to assign the x -coordinates of $\swarrow(v)$ and $\searrow(v)$. We are going to perform this assignment based on $\Delta(v_b)$ and $\Delta(v_g)$, which have already been drawn in R_{i-1} . Indeed, since the blue edge (v_b, v) and the green edge (v_g, v) are entering v in $\text{DAG}_r(T)$, we have that $\tau'(v_b) < \tau'(v)$ and $\tau'(v_g) < \tau'(v)$.

Before describing the assignment of the x -coordinates of $\swarrow(v)$ and $\searrow(v)$, we discuss some properties of R_{i-1} . First, by condition (i) of ADT-labeling, we have that $\tau(v_b) \leq \tau(v)$ and $\tau(v_g) \leq \tau(v)$, and thus the horizontal side of $\Delta(v)$ will not lie below the ones of $\Delta(v_b)$ and $\Delta(v_g)$. Also, we assume that the following two invariants hold in R_{i-1} and we will show that they also hold in R_i after drawing $\Delta(v)$:

- (i) The y -coordinates of $\nearrow(v_b)$ and $\nearrow(v_g)$ are both greater than or equal to $\tau(v)$.
- (ii) Let $v_1 = X_b, \dots, v_q = X_g$ be the path along the outer face of G_{i-1} . Then $\nearrow(v_1), \dots, \nearrow(v_q)$ have increasing x -coordinates in R_{i-1} .

The two invariants imply in particular that the horizontal line $y = \tau(v)$ intersects both, $\Delta(v_b)$ and $\Delta(v_g)$, and that $\Delta(v_b)$ is to the left of $\Delta(v_g)$. Thus, $\Delta(v)$ can only touch $\Delta(v_b)$ and $\Delta(v_g)$ if $\swarrow(v)$ and $\searrow(v)$ are the intersection point of the line $y = \tau(v)$ with $\triangleleft(v_b)$ and $\nearrow(v_g)$, respectively. This implies the uniqueness of the RT-representation, under the constraints imposed by the function τ and the given RT-representation R_o of the outer face. We thus assign the x -coordinates of $\swarrow(v)$ and $\searrow(v)$ accordingly, hence obtaining a representation R_i . In the following, we prove that R_i is actually an RT-representation of G_i corresponding to the Schnyder wood T .

Since R_i contains R_{i-1} , which is an RT-representation of G_{i-1} , we only need to consider the touchings between v and its neighbors in G_i . Since vertices of G are processed according to a topological ordering τ' of $\text{DAG}_r(T)$, such neighbors of v are exactly v_b, v_g , and each vertex u such that $u_r = v$. By construction, $\swarrow(v)$ and $\searrow(v)$ touch $\triangleleft(v_b)$ and $\nearrow(v_g)$, respectively. Next, we prove that $\nearrow(u)$ touches $\triangleleft(v)$ for each vertex u such that $u_r = v$. Namely, by construction, $\nearrow(u)$ has y -coordinate equal to $\tau(v)$, so it suffices to show that $\nearrow(u)$ is between $\swarrow(u_r)$ and $\searrow(u_r)$. This is obvious if $u_r = X_r$. Otherwise, this directly follows from invariant (ii), since u appears between v_b and v_g on the X_b - X_g -path along the outer face of G_{i-1} . Thus, all corners touch the correct side of another triangle as required by the Schnyder wood T .

Then, we show that the horizontal side of $\Delta(v)$ has positive length. This is clear if $\tau(v)$ is strictly greater than both $\tau(v_g)$ and $\tau(v_b)$. So assume first that $\tau(v_b) < \tau(v) = \tau(v_g)$. Then, by condition (ii) of ADT-labeling, there is a vertex u such that $\langle v, v_g, u \rangle$ is a clockwise facial cycle. It follows that (u, v) is an incoming red edge of v in T and thus $\nearrow(u)$ lies between $\Delta(v_b)$ and $\Delta(v_g)$ on the horizontal line $y = \tau(v)$, as discussed above. Since the horizontal side of $\Delta(u)$ has a positive length in R_{i-1} and

since $\tau(v_b) < \tau(v)$, the vertical side of $\Delta(v_b)$ must be strictly to the left of $\overrightarrow{\mathcal{A}}(u)$, and thus strictly to the left of $\overrightarrow{\mathcal{A}}(v_g)$. The case $\tau(v_b) = \tau(v) > \tau(v_g)$ is analogous. Finally, we consider the case $\tau(v_b) = \tau(v) = \tau(v_g)$. By condition (iii) of ADT-labeling, there exist two distinct vertices u_1 and u_2 such that $\langle v, v_g, u_1 \rangle$ is a clockwise facial cycle and $\langle v, v_b, u_2 \rangle$ is a counter-clockwise facial cycle. Since the horizontal side of $\Delta(u_1)$ and $\Delta(u_2)$ have positive length in R_{i-1} , the right corner of $\Delta(v_b)$ and the left corner of $\Delta(v_g)$ cannot coincide.

This concludes the proof that R_i is an RT-representation of G_i . We conclude by showing that the two invariants are maintained in R_i .

Invariant (i) is fulfilled: We show that the top corner of $\Delta(v_b)$ has y-coordinate greater than or equal to $\tau(v)$. The arguments for $\Delta(v_g)$ are analogous. If $v_b = X_b$, this follows from the fact that $\overrightarrow{\mathcal{A}}(X_b)$ has y-coordinate greater than or equal to $\tau(X_r)$ in R_o .

Otherwise, recall that the y-coordinate of $\overrightarrow{\mathcal{A}}(v_b)$ has been set equal to $\tau(r)$, where r is the neighbor of v_b such that edge (v_b, r) of $\text{DAG}_r(T)$ is red. Let w_1, \dots, w_k (with $w_1 = v$ and $w_k = r$) be the neighbors of v_b such that edges $(v_b, w_1), \dots, (v_b, w_k)$ appear in this counter-clockwise order around v_b . See the figure to the right. Since (v_b, w_1) is blue and entering v_b in T , while (v_b, w_k) is red and exiting v_b in T , we have that each edge (v_b, w_i) , with $2 \leq i \leq k - 1$, is blue and entering v_b in T .

It follows that the edge $e = (w_j, w_{j+1})$, for $j = 1, \dots, k - 1$ is the next edge incident to w_j in clockwise direction after an outgoing blue edge. Thus, e is either red and exiting w_j in T or green and entering w_j in T . Hence, w_1, \dots, w_k form a directed path from v_b to r in $\text{DAG}_r(T)$, where red edges maintain their orientation while green edges are reversed. Hence, $\tau(r) \geq \tau(v)$. Thus, $\overrightarrow{\mathcal{A}}(v_b)$ has y-coordinate larger than or equal to $\tau(v)$, as desired.

Invariant (ii) is fulfilled: Let $P_{i-1} : v_1 = X_b, \dots, v_q = X_g$ be the path along the outer face of G_{i-1} . Since R_{i-1} satisfies invariant (ii), we have that $\overrightarrow{\mathcal{A}}(v_1), \dots, \overrightarrow{\mathcal{A}}(v_q)$ have increasing x-coordinates in R_{i-1} . Let $1 \leq \ell < k \leq q$ be such that $v_b = v_j$ and $v_g = v_k$. Then, the path P_i along the outer face of G_i is obtained from P_{i-1} by replacing the sequence v_j, \dots, v_k by v_j, v, v_k . Since we place v between $v_j = v_b$ and $v_k = v_g$, the invariant holds in R_i .

As both invariants trivially hold in the given drawing of $\Delta(X_b)$ and $\Delta(X_g)$, the lemma follows. □

4 Geometric Tools

In this section, we provide geometric lemmata that will be exploited in the subsequent sections. We first show that the incidence of a point and a line segment is maintained during a linear morph if the line segment is moved in parallel (with a possible stretch, but keeping the orientation) or the ratio with which the point cuts the segment is maintained; see Fig. 8.

Lemma 4.1 *For $i = 0, 1$ let p_i, q_i be two points in the plane and let $x_i \in \overline{p_i q_i}$. For $0 < t < 1$, further let $p_t = (1 - t)p_0 + tp_1$ and $q_t = (1 - t)q_0 + tq_1$. Then, $x_t = (1 - t)x_0 + tx_1 \in \overline{p_t q_t}$ if*

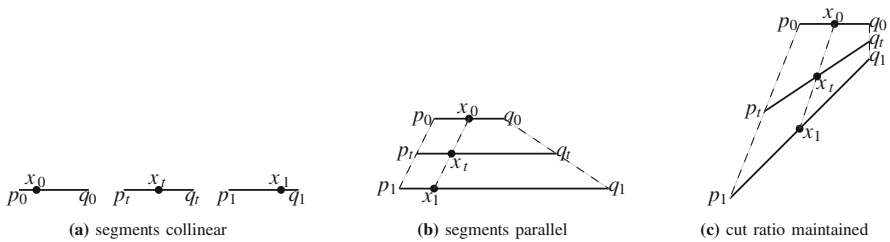


Fig. 8 Morphing a segment and a point

- $\overline{p_0q_0}$ and $\overline{p_1q_1}$ are parallel with the same direction, or
- x_0 cuts $\overline{p_0q_0}$ with the same ratio as x_1 cuts $\overline{p_1q_1}$.

Moreover, in both cases, if $x_t = p_t$ for some $t \in [0, 1]$ then $x_0 = p_0$ and $x_1 = p_1$.

Proof Assume first that $\overline{p_0q_0}$ and $\overline{p_1q_1}$ are parallel. If $\overline{p_0q_0}$ and $\overline{p_1q_1}$ are collinear, we may assume that they are both contained in the x-axis, that $p_i, q_i, i = 0, 1$, are real numbers, and that $p_0 < q_0$. Since $\overline{p_0q_0}$ and $\overline{p_1q_1}$ have the same direction, this implies that $p_1 < q_1$. Since $x_i, i = 0, 1$, is a point in $\overline{p_iq_i}$, it follows that $p_i \leq x_i \leq q_i$. Hence, we get for $t \in [0, 1]$ that

$$\underbrace{(1-t)p_0 + tp_1}_{p_t} \leq \underbrace{(1-t)x_0 + tx_1}_{x_t} \leq \underbrace{(1-t)q_0 + tq_1}_{q_t},$$

where equality holds if and only if $x_0 = p_0$ and $p_1 = x_1$, or $x_0 = q_0$ and $x_1 = q_1$, respectively.

If $\overline{p_0q_0}$ and $\overline{p_1q_1}$ are parallel with the same direction but not collinear, then the polygon $\langle p_0, q_0, q_1, p_1 \rangle$ is convex. Thus, $\overline{x_0x_1}$ must intersect $\overline{p_1q_1}$, for any t . Also, $\overline{p_tq_t}$ and x_t both lie on the same line ℓ_t . More precisely, let d be the distance between the lines through segments $\overline{p_0q_0}$ and $\overline{p_1q_1}$. Then, ℓ_t is the line with distance td from $\overline{p_0q_0}$. Moreover, due to the convexity of $\langle p_0, q_0, q_1, p_1 \rangle$, we have that $x_t = p_t$ implies $x_0 = p_0$ and $x_1 = p_1$.

Finally, if x_0 cuts $\overline{p_0q_0}$ with the same ratio λ as x_1 cuts $\overline{p_1q_1}$, then it follows that $x_t = (1-t)((1-\lambda)p_0 + \lambda q_0) + t((1-\lambda)p_1 + \lambda q_1) = (1-\lambda)p_t + \lambda q_t \in \overline{p_tq_t}$. Moreover, $x_t = p_t$ if and only if $\lambda = 0$, and, thus, $x_0 = p_0$ and $x_1 = p_1$. \square

Lemma 4.1 implies the following sufficient criterion for a linear morph. For an illustration of the special shape assumed for the outer face in the following lemma see, e.g., Fig. 2.

Lemma 4.2 *Let R_0 and R_1 be two RT-representations of a triangulation G corresponding to the same Schnyder wood such that the triangles of the outer face pairwise touch in their corners. The pair $\langle R_0, R_1 \rangle$ defines a linear morph if, for any two adjacent vertices u and v such that a corner $c_i(v)$, $i \in \{0, 1\}$, of v touches a side $s_i(u)$ of u , where $c \in \{\nearrow, \searrow, \perp\}$ and $s \in \{\triangleleft, \triangleright, \nearrow\}$, one of the following holds:*

- (i) $s_0(u)$ and $s_1(u)$ are parallel.

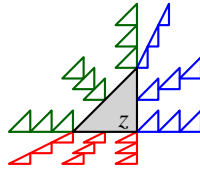


Fig. 9 The three quadrants containing triangles on a red, green, or blue path to z

(ii) $c_0(v)$ cuts $s_0(u)$ with the same ratio as $c_1(v)$ cuts $s_1(u)$.

Proof Let R_t be the representation at time instant t of the linear morph from R_0 to R_1 , with $t \in [0, 1]$, i.e., the set of triangles obtained by interpolating the corners of each triangle in R_0 to R_1 . It suffices to show that R_t is an RT-representation of G .

We start by proving that, for every vertex u of G , the triangle $\Delta_t(u)$ representing u in R_t is the lower-right half of an axis-parallel rectangle with positive area. Consider the triangles $\Delta_0(u)$ and $\Delta_1(u)$ representing u in R_0 and R_1 , respectively. Since $\lrcorner_1(u)$ and $\lrcorner_2(u)$ are vertical segments with $\nearrow_1(u)$ lying above $\lrcorner_1(u)$, with $i = 0, 1$, we have that $\lrcorner_t(u)$ is a vertical segment with $\nearrow_t(u)$ lying above $\lrcorner_t(u)$. A similar argument applies to prove that $\lrcorner_t(u)$ is a horizontal segment with $\lrcorner_t(u)$ lying to the left of $\lrcorner_t(u)$. Since all these segments have positive length, the claim follows.

Next, we prove that R_t is an RT-representation of G , i.e., we show that any two triangles touch in R_t if and only if the corresponding vertices of G are adjacent, and that no two triangles share more than one point.

First, consider two vertices u and w that are adjacent in G . We show that $\Delta_t(u)$ and $\Delta_t(w)$ touch in exactly one point. Let $c_0(u)$ with $c \in \{\nearrow, \lrcorner, \lrcorner\}$ and $s_0(w)$ with $s \in \{\lrcorner, \lrcorner, \lrcorner\}$ be the corner of $\Delta_0(u)$ and the side of $\Delta_0(w)$, respectively, that touch in R_0 . Since R_0 and R_1 correspond to the same Schnyder wood, and since the triangles of the outer face pairwise touch in their corners, we have that the corner $c_1(u)$ of $\Delta_1(u)$ touches the side $s_1(w)$ of $\Delta_1(w)$ in R_1 . This, together with Lemma 4.1, implies that the corner $c_t(u)$ of $\Delta_t(u)$ touches the side $s_t(w)$ of $\Delta_t(w)$ in R_t . The fact that no other points are shared between $\Delta_t(u)$ and $\Delta_t(w)$ derives from the possible corner-side pairs (c, s) that may appear in an RT-representation. This also implies that R_t induces the same Schnyder wood as R_0 and R_1 .

Second, consider two vertices u and w that are not adjacent in G . We show that $\Delta_t(u)$ and $\Delta_t(w)$ do not share any point in R_t . We are going to exploit the following property of a Schnyder wood T of G [5, 27, 46]: Let T_r, T_g, T_b , respectively, be the subtree of T induced by the red, green, and blue edges, respectively. There exists a vertex z , possibly $z = w$, such that T_i contains a path $P_{u,z}$ from u to z and T_j contains a path $P_{w,z}$ from w to z , for some $i \neq j \in \{r, g, b\}$. We will show that $\Delta_t(u)$ and $\Delta_t(w)$ are in different quadrants of $\lrcorner_t(z)$. See Fig. 9 for an illustration.

Consider a path P to z such that every edge has the same color. Then any corner-side pair determined by any edge in P is of the same type, more precisely, of type (\lrcorner, \lrcorner) if P is green, of type (\lrcorner, \lrcorner) if P is blue, and of type (\nearrow, \lrcorner) if P is red. Let a be a vertex. If there is a green a - z -path then $\Delta_t(a)$ is in the upper left quadrant of $\lrcorner_t(z)$, including the boundary above $\nearrow_t(z)$ or to the left of $\lrcorner_t(z)$. If there is a blue a - z -path then $\Delta_t(a)$ is in the upper right quadrant of $\lrcorner_t(z)$, including the boundary

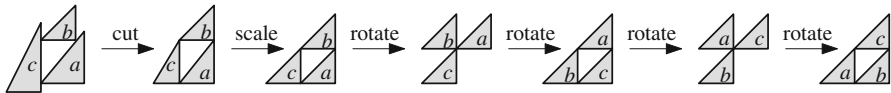


Fig. 10 Morphing an RT-representation of a triangle to a labeled canonical form: First, cut the extruding parts of the triangles, maintaining the slopes of the diagonal sides. Then, scale the triangles such that the horizontal and vertical sides have length one. Finally, keep rotating the triangles until the topmost vertex is as desired

between $\nearrow_T(z)$ and $\searrow_T(z)$. Finally, if there is a red a - z -path then $\Delta_T(a)$ is in the lower-left quadrant of $\searrow_T(z)$, including the boundary between $\swarrow_T(z)$ and $\searrow_T(z)$. The only three points where triangles of these three regions could intersect are the three corners of $\Delta_T(z)$. Assume that a corner of $\Delta_T(u)$ and a corner of $\Delta_T(w)$ coincide with the same corner of $\Delta_T(z)$. But then the last statement of Lemma 4.1 would imply that the same corners would also coincide in R_0 and R_1 —contradicting that u and w were not adjacent. □

5 A Morphing Algorithm

In this section, we prove that the necessary conditions in Theorem 3.4 are also sufficient and show how to construct a piecewise linear morph if the conditions are fulfilled.

Theorem 5.1 (sufficient condition) *Let R_1 and R_2 be two RT-representations of an n -vertex plane triangulation G corresponding to the Schnyder woods T_1 and T_2 , respectively. If T_2 can be obtained from T_1 by a sequence of ℓ facial flips, then there exists a piecewise linear morph between R_1 and R_2 of length $\mathcal{O}(n + \ell)$. Such a morph can be computed in $\mathcal{O}(n(n + \ell))$ time, provided that the respective sequence of ℓ facial flips is given.*

Since there is always a piecewise linear morph between two RT-representations of a plane triangle (see Fig. 10), we will assume that G has at least four vertices. The fact that T_1 can be obtained from T_2 by a sequence of facial flips implies in particular that the topmost vertex, which always coincides with X_r , is the same in R_1 and R_2 .

In Sect. 5.1, we introduce our main procedure ADJUST, which moves a triangle in an RT-representation along an incident diagonal and adjusts the remaining triangles so that the result is a linear morph. Repeatedly applying ADJUST, we first morph R_1 to a non-degenerate RT-representation that still corresponds to T_1 (Sect. 5.3); then, we perform a sequence of linear morphs to geometrically realize the ℓ facial flips (Sect. 5.2), hence obtaining an RT-representation corresponding to T_2 , which we finally morph to R_2 (Sect. 5.3). See Fig. 11 for an illustration.

5.1 Moving a Triangle Along a Diagonal

Let $G = (V, E)$ be a plane triangulation and let R be an RT-representation of G corresponding to a Schnyder wood T of G . Given an inner vertex σ of G and a real value y with some properties, ADJUST computes a new RT-representation R' of G

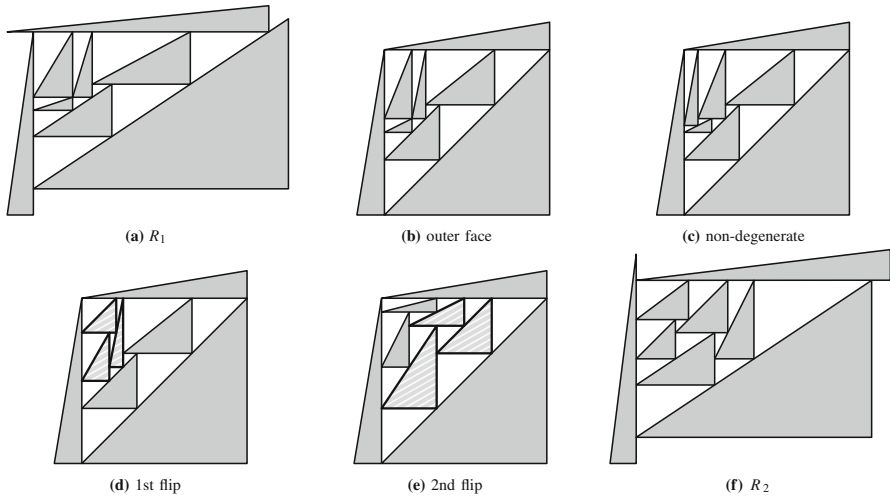


Fig. 11 Construction pipeline: First, **(b)** we trim the outer face into a canonical form (three steps) and **(c)** make the inner faces non-degenerate (one step per face). Then, **(d)** + **(e)** we perform the facial flips on the faces indicated by striped triangles (two steps per flip). Finally, **(f)** we morph to the target RT-representation (linear number of steps)

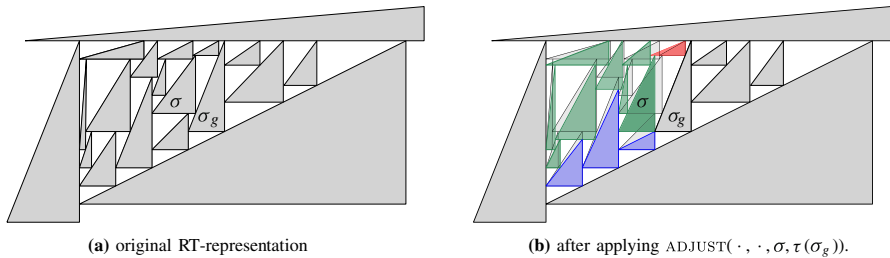


Fig. 12 Moving $\perp(\sigma)$ down along $\nearrow(\sigma_g)$. The gray triangles are not changed at all, the y-coordinates τ of the bases of the light green triangles is adjusted such that the ratio with which the incident diagonal is cut is maintained. The y-coordinates of the bases of the light blue and light red triangles do not change—however their height (light blue) or width (light red) changes

corresponding to T in which $\triangleleft(\sigma)$ has y-coordinate y and $\triangleleft(\sigma_g)$ remains unchanged, such that $\langle R, R' \rangle$ is a linear morph.

To achieve this goal, the y-coordinate of $\triangleleft(v)$, for some vertex $v \neq \sigma$, may also change; however, the ratio with which $\perp(v)$ cuts $\nearrow(v_g)$ does not change, thus satisfying **(ii)** of Lemma 4.2. See Fig. 12 for an illustration. The y-coordinates of the horizontal sides are encoded by a new ADT-labeling τ of G , and R' is the unique RT-representation $RT(T, \tau, R_o)$ of G that is obtained by applying Lemma 3.6 with input G, T, τ , and the representation R_o of the outer face of G in R .

For a vertex $w \in V$, we let $\text{top}(w)$ denote the y-coordinate of $\nearrow(w)$; recall that, in our construction, we have $\text{top}(w) = \tau(w_r)$, if w is an inner vertex. Also, let v_1, \dots, v_ℓ be the neighbors of w such that $\perp(v_1), \dots, \perp(v_\ell)$ appear in this order from $\searrow(w)$ to

$\nearrow(w)$ along $\swarrow(w)$. For a fixed $i \in \{1, \dots, \ell\}$, we say that moving $\perp\!\!\!\downarrow(v_i)$ to $y_0 \in \mathbb{R}$ respects the order along $\swarrow(w)$ if

- (i) $i = 1$ and $\tau(w) \leq y_0 < \tau(v_2)$ (where equality is only allowed if $\swarrow(v_1)$ does not lie on $\swarrow(w_b)$),
- (ii) $i = 2, \dots, \ell - 1$ and $\tau(v_{i-1}) < y_0 < \tau(v_{i+1})$, or
- (iii) $i = \ell$ and $\tau(v_{i-1}) < y_0 \leq \text{top}(w)$ and $y_0 < \text{top}(v_\ell)$.

Further, for a vertex v , we consider the ratio $\lambda(v)$ with which $\perp\!\!\!\downarrow(v)$ cuts the incident diagonal side, i.e., $\lambda(v) = (\tau(v) - \tau(v_g)) / (\text{top}(v_g) - \tau(v_g))$, if either v is an inner vertex or $v \in \{X_b, X_r\}$, $\perp\!\!\!\downarrow(v)$ is on $\swarrow(X_g)$, and $v_g := X_g$.

For the vertex σ and the y-coordinate y that are part of the input of ADJUST, we assume that moving σ to y respects the order along $\swarrow(\sigma_g)$. This allows to set $\tau(\sigma) \leftarrow y$ without changing the contact point between $\perp\!\!\!\downarrow(v)$ and $\swarrow(\sigma_g)$ for any other vertex v such that $v_g = \sigma_g$. On the other hand, setting $\tau(\sigma) \leftarrow y$ may have other implications on the neighbors of σ , as follows:

- Type 1. For every vertex v such that $\sigma = v_g$, the value of $\tau(v)$ has to be modified to ensure that the ratio $\lambda(v)$ with which $\perp\!\!\!\downarrow(v)$ cuts $\swarrow(\sigma)$ is maintained;
- Type 2. for every vertex u such that $\sigma = u_r$, we have to set $\text{top}(u) = y$ to maintain the contact between $\Delta(u)$ and $\Delta(\sigma)$.

Let v and u be two vertices that have been modified according to Types 1 and 2, respectively. Since these modifications may change the diagonal side of $\Delta(v)$ and $\Delta(u)$, they may trigger analogous implications for the neighbors of v and u . Observe that, since the y-coordinate of $\swarrow(u)$ is not changed, only a Type 1 implication may be triggered for the neighbors of u . Further, the two implications correspond to following either a red or a green edge, respectively, in reverse direction with respect to the one in T . Hence, the vertices whose triangles may need to be adjusted are those that can be reached from the vertex σ by a reversed directed path in T using only red and green edges, but no two consecutive red edges; see Fig. 13. Note that, since the green and the red edges have opposite orientation in T and in $\text{DAG}_b(T)$, which is acyclic, this implies that ADJUST terminates.

The procedure ADJUST (see Algorithm 1 for its pseudo-code and Fig. 12 for an illustration) first finds all the triangles that may need to be adjusted, by performing a simple graph search from σ following the above described paths of red and green edges. In a second pass, it performs the adjustment of each triangle $\Delta(w)$, by modifying $\tau(w)$ so that $\lambda(w)$ is maintained for $w \neq \sigma$. We ensure that the new value of $\tau(w)$ is computed only after the triangle $\Delta(w_g)$ has already been adjusted.

Lemma 5.2 *Let R_1 be an RT-representation of a plane triangulation $G = (V, E)$ corresponding to the Schnyder wood T and let the y-coordinate of $\swarrow_1(v)$ be $\tau_1(v)$, $v \in V$. Let $\sigma \in V$ be an inner vertex and let $y \in \mathbb{R}$ be such that moving σ to y respects the order along $\swarrow(\sigma_g)$. Let τ_2 be the output of $\text{ADJUST}(\tau_1, T, \sigma, y)$. The following conditions hold.*

- (i) $\tau_2(\sigma) = y$.
- (ii) $\lambda(v)$ is maintained for any vertex $v \neq \sigma$.
- (iii) τ_2 is an ADT-labeling of $\text{DAG}_r(T)$.

Algorithm 1: Pseudo-code of procedure ADJUST

Input : RT-representation R of a plane triangulation $G = (V, E)$ with $\angle(v)$ on $\tau(v)$, $v \in V$, and Schnyder wood T . A vertex $\sigma \in V$, a real number $y \in \mathbb{R}$ such that moving σ to y respects the order along $\nearrow(\sigma_g)$.

Output: ADT-labeling τ of $\text{DAG}_r(T)$ with (i) $\tau(\sigma) = y$, (ii) the ratio $\lambda(v)$ is maintained for any vertex $v \neq \sigma$, and (iii) the triangle $\Delta(\sigma_g)$ is the same in R and $\text{RT}(T, \tau, R_o)$, where R_o is the representation of the outer face in R .

Data: Stack S ; Boolean $v.\text{RED}$, $v.\text{GREEN}$, for each $v \in V$ initialized to FALSE, describing whether v was found by traversing a red edge, or a green edge, or both (TRUE in the first round and FALSE in the second).

```

ADJUST( $y$ -coordinates  $\tau$ , Schnyder wood  $T$ , vertex  $\sigma$ , real  $y$ )
  for  $u \in V$  do
     $\lambda(u) \leftarrow (\tau(u) - \tau(u_g)) / (\text{top}(u_g) - \tau(u_g))$ 
   $\tau(\sigma) \leftarrow y$ ;
  for  $i = 1, 2$  do
     $S.\text{PUSH}(\sigma)$ ;
    for each incoming red edge  $(u, \sigma)$  of  $\sigma$  do
       $u.\text{RED} \leftarrow \neg u.\text{RED}$ ; /* true in first pass, false in second */
      if  $\neg u.\text{GREEN}$  then /* always fulfilled in first pass */
         $S.\text{PUSH}(u)$ ;
    while  $S \neq \emptyset$  do
       $w \leftarrow S.\text{POP}$ ;
      for each incoming green edge  $(v, w)$  of  $w$  do
        if  $i = 2$  then
           $\tau(v) \leftarrow \lambda(v) \cdot (\tau(w_r) - \tau(w)) + \tau(w)$ ; /*  $\tau(w_r) = \text{top}(w)$  */
           $v.\text{GREEN} \leftarrow \neg v.\text{GREEN}$ ;
          if  $\neg v.\text{RED}$  then
             $S.\text{PUSH}(v)$ ;
        for each incoming red edge  $(u, v)$  of  $v$  do
           $u.\text{RED} \leftarrow \neg u.\text{RED}$ ;
          if  $\neg u.\text{GREEN}$  then
             $S.\text{PUSH}(u)$ ;

```

(iv) The morph between R_1 and $R_2 = \text{RT}(T, \tau_2, R_o)$ is linear, where $R_o = \Delta_1(X_b) \cup \Delta_1(X_g) \cup \Delta_1(X_r)$.

Proof The fact that $\tau_2(\sigma) = y$ and that $\lambda(v)$ is maintained for any vertex $v \neq \sigma$ follows by construction. This establishes conditions (i) and (ii). To prove that τ_2 is an ADT-labeling, condition (iii), we first determine a cycle C' bounding a subgraph of G containing all the vertices whose τ might be modified by procedure ADJUST (see Fig. 13). We then prove condition (iii) by induction on a suitable ordering of the edges in $\text{DAG}_r(T)$. We finally exploit Lemma 4.2 to establish that $\langle R_1, R_2 \rangle$ is a linear morph, i.e., condition (iv). □

A cycle C' enclosing all vertices where τ might change. Let u be the neighbor of σ following σ_g in clockwise order around σ . Observe that either $\sigma = u_r$ or $u = \sigma_b$. Consider the blue $u-X_b$ -path p_b and the red $\sigma-X_r$ -path p_r of G (see Fig. 13). Let C' be

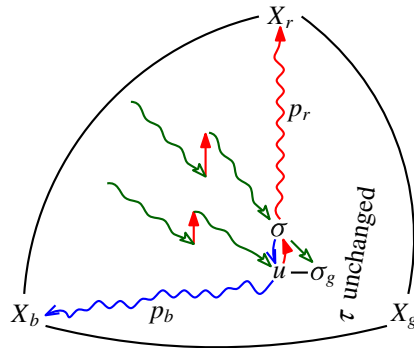


Fig. 13 Let u be the neighbor of σ following σ_g in clockwise order. Then, the cycle C' composed of the blue u - X_b -path p_b , the edge $\{u, \sigma\}$, the red σ - X_r -path p_r , and the edge $\{X_r, X_b\}$ encloses all vertices for which τ is changed. Vertex σ is the only vertex on C' for which τ is changed

the cycle composed by $X_b, p_b, u, \sigma, p_r, X_r$. Let $v \neq \sigma$ be a vertex such that $\tau_2(v) \neq \tau_1(v)$. We claim that v lies in the interior of C' . In fact, ADJUST sets $\tau_2(v) \neq \tau_1(v)$ only if there exists in $\text{DAG}_b(T)$ a directed red-green-path p with no two consecutive red edges starting at σ and ending with a green edge at v . This is due to the fact that, when processing a vertex w , procedure ADJUST might choose to process a neighbor v of w only if T contains the green edge (v, w) and then it might choose to process a neighbor u of v only if T contains the red edge (u, v) . Recall that green and red edges have opposite orientation in T and $\text{DAG}_b(T)$.

Note that p starts at σ , which lies along C' and, after possibly reaching u via a red edge, it necessarily enters the interior of C' via a green edge. In the following steps p can reach again a vertex z of C' ; however this can only happen if z belongs to p_b and it is reached via a red edge. This implies that the next edge of p is green and hence p enters again the interior of C' . Thus, v lies in the interior of C' .

τ_2 is an ADT-labeling. If $y = \tau_1(\sigma)$ then $\tau_1 = \tau_2$ is an ADT-labeling. Otherwise, distinguishing the cases $y < \tau_1(\sigma)$ and $y > \tau_1(\sigma)$ we will prove by induction on a suitable ordering of the edges in $\text{DAG}_r(T)$ the following property.

Property DTL: $\tau_2(v) \leq \tau_2(w)$ for any edge (v, w) of $\text{DAG}_r(T)$ where equality may only hold if

- (i) $\tau_1(v) = \tau_1(w)$,
- (ii) $w = \sigma, v = \sigma_g$, and $\langle \sigma, \sigma_g, v_b \rangle$ is a clockwise oriented facial cycle in T , or
- (iii) $v = \sigma = w_b$ and $\langle w, \sigma, \sigma_g \rangle$ is a counter-clockwise oriented facial cycle in T .

This immediately establishes condition (i) of ADT-labeling for τ_2 . In order to prove (ii), let $e = (v, w)$ be an edge of $\text{DAG}_r(T)$ with $\tau_2(v) = \tau_2(w)$. We have to show that the edge between v and w in the Schnyder wood T is green and belongs to a clockwise oriented facial cycle, or blue and belongs to a counter-clockwise oriented facial cycle. If $\tau_1(v) = \tau_1(w)$, this follows immediately from the fact that τ_1 is an ADT-labeling of $\text{DAG}_r(T)$. Otherwise, conditions (ii) and (iii) of Property DTL immediately guarantee the right color of the edge and the right direction of the facial cycle. Recall that green and blue edges have different directions in T and in $\text{DAG}_r(T)$.

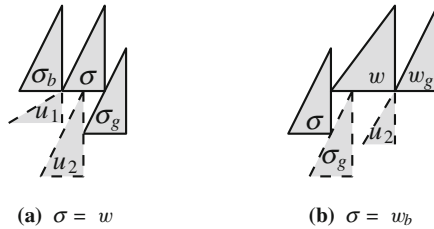


Fig. 14 If the horizontal sides of the solid triangles are on one line in R_2 then the two dashed triangles closing a counter-clockwise facial cycle with (w, w_b) and a clockwise facial cycle with (w, w_g) , respectively, are distinct. Situation drawn with respect to R_1

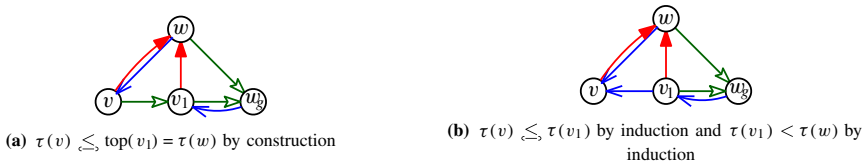


Fig. 15 Property DTL in the case $y < \tau(\sigma)$

Finally, we have to prove that condition (iii) of an ADT-labeling is fulfilled. To this end, consider a vertex w with $\tau_2(w_b) = \tau_2(w) = \tau_2(w_g)$ and let u_1 and u_2 be two vertices such that $\langle w, w_g, u_1 \rangle$ is a clockwise facial cycle and $\langle w, w_b, u_2 \rangle$ is a counter-clockwise facial cycle. We have to show that $u_1 \neq u_2$. If neither (ii) nor (iii) of Property DTL holds for the edges (w_b, w) and (w_g, w) of $\text{DAG}_r(T)$, i.e., if neither $w = \sigma$ nor $w_b = \sigma$, then condition (i) of Property DTL implies $\tau_1(w_b) = \tau_1(w) = \tau_1(w_g)$. Since τ_1 is an ADT-labeling, it follows that $u_1 \neq u_2$. So assume that $\sigma \in \{w, w_b\}$. We distinguish the last two cases of Property DTL (see Fig. 14).

Assume first that $\sigma = w$ (condition (ii) of Property DTL) and the clockwise facial cycle incident to (w, w_g) in T is $\langle w, w_g, u_2 \rangle = \langle \sigma, \sigma_g, u_2 \rangle$ for some vertex u_2 . This implies that (σ_g, u_2) is blue, (u_2, σ) is red, and $y = \tau_2(\sigma) = \tau_2(w) = \tau_2(w_g) = \tau_2(\sigma_g) = \tau_1(\sigma_g) = \tau_1(w_g)$. Since in this case neither (ii) nor (iii) of Property DTL holds for the edge (w_b, w) of $\text{DAG}_r(T)$, $\tau_2(w_b) = \tau_2(w)$ implies $\tau_1(w_b) = \tau_1(w)$. The vertex $u_1 \in V$ for which $\langle w, w_b, u_1 \rangle$ is a counter-clockwise facial cycle fulfills $\mathcal{A}_1(u_1) = \mathcal{A}_1(w_b) = \mathcal{A}_1(w)$. Since moving σ to $y = \tau_2(\sigma_g) = \tau_1(\sigma_g)$ respects the order along $\mathcal{A}(\sigma_g)$ (condition (i)), it follows that $\mathcal{A}_1(\sigma)$ is not on $\mathcal{A}_1(u_2)$. Thus $u_1 \neq u_2$.

Assume now that $\sigma = w_b$ (condition (iii) of Property DTL) and that $\langle w, \sigma, \sigma_g \rangle = \langle w, w_b, \sigma_g \rangle$ is the counter-clockwise oriented facial cycle in T incident to the edge (w, w_b) , i.e., $u_1 = \sigma_g$. In this case w and w_g are outside the cycle C' and, thus, $\tau_1(w) = \tau_2(w)$ and $\tau_1(w_g) = \tau_2(w_g)$. Since moving σ to $y = \tau_2(\sigma) = \tau_2(w_b) = \tau_2(w) = \tau_1(w) = \text{top}(\sigma_g)$ respects the order along $\mathcal{A}(\sigma_g)$ (condition (iii)), it follows that $\mathcal{A}_1(w)$ is not on $\mathcal{A}_1(\sigma_g)$ and $\mathcal{A}_1(\sigma)$ is strictly above $\mathcal{A}_1(\sigma_g)$. It follows that $\tau_1(w) = \tau_2(w) = \tau_2(w_g) = \tau_1(w_g)$. Thus the clockwise facial cycle incident to (w, w_g) is $\langle w, w_g, u_2 \rangle$ with $\mathcal{A}_1(u_2) = \mathcal{A}_1(w) \neq \mathcal{A}_1(\sigma_g)$. It follows that $u_1 = \sigma_g \neq u_2$.

It remains to show Property DTL. In order to do so, we will use induction. Observe that for some already considered edge $e = (v, w)$ of $\text{DAG}_r(T)$ the inductive hypothesis implies in particular that $\tau_1(v) = \tau_1(w)$ if $\tau_2(v) = \tau_2(w)$ unless $w = \sigma$ and e is green, or $v = \sigma$ and e is blue. This implies in particular that $\tau_2(v) < \tau_2(w)$ if e is red.

Case $y < \tau_1(\sigma)$: Note that, in this case, procedure ADJUST does not increase τ for any vertex, that is, $\tau_2(v) \leq \tau_1(v)$ for every vertex v . We use induction on the following lexicographical ordering of the edges of $\text{DAG}_r(T)$: Consider any ordering $<$ extending the partial order given by $\text{DAG}_r(T)$. An edge (v_1, w_1) is considered before an edge (v_2, w_2) if $w_1 < w_2$, or $w_1 = w_2 =: w$ and v_1 comes before v_2 in the clockwise order around w starting from (w_g, w) .

Let (v, w) be an edge of $\text{DAG}_r(T)$. Since τ_1 is an ADT-labeling of $\text{DAG}_r(T)$, it follows that $\tau_1(v) \leq \tau_1(w)$. Moreover, τ did not increase for any vertex. Thus, if $\tau(w)$ does not change then⁴ $\tau_2(v) \leq \tau_1(v) \leq \tau_1(w) = \tau_2(w)$ for any descendant v of w . This is especially true if w is the first vertex with incoming edges with respect to $<$, i.e., the first vertex after X_b and X_g .

Let now (v, w) be an edge of $\text{DAG}_r(T)$ such that $\tau(w)$ changes. Assume first that (v, w) is a green edge, i.e., $v = w_g$. There are two cases. Either $w = \sigma$, and $\tau_2(v) = \tau_2(\sigma_g) = \tau_1(\sigma_g) \leq y = \tau_2(\sigma) = \tau_2(w)$ (where equality is only allowed if $\perp_b(\sigma)$ is the bottommost corner on $\angle(\sigma_g)$, and $\angle(\sigma_g)$ and $\angle(\sigma)$ are not both on the vertical side of the same triangle, i.e., if (σ, σ_g, v_b) is an oriented face in T). Or $\tau(w)$ is changed according to the ratio on $\angle(v)$ and, thus, the relationship $\tau(v) \leq \tau(w)$ is maintained.

Consider now the case that (v, w) is an incoming red edge of w or an outgoing (in T) blue edge of w . Let $v = v_0, v_1, \dots, v_k = w_g$ be the neighbors of w in counter-clockwise order from v to w_g . Observe that (v_i, w) , $i = 1, \dots, k - 1$, (if any) are red. By induction, we have $\tau_2(v_i) \leq \tau_2(w)$, $i = 1, \dots, k$. Observe further that for any $i = 1, \dots, k$ either (v_{i-1}, v_i) is a green edge or (v_i, v_{i-1}) is a blue edge. See Fig. 15.

Assume first that $k = 1$, i.e., $v_1 = w_g$. First observe that $\tau_2(v) \leq \tau_2(w_g)$ by induction, if (w_g, v) is blue, and by construction, if (v, w_g) is green. If $w = \sigma$, then $\tau_2(v) \leq \tau_1(v) < y = \tau_2(\sigma)$, since moving $\perp_b(w)$ to y must respect the order along $w_g = \sigma_g$ and $\tau_1(v) < \tau_1(w)$. If $w \neq \sigma$ and (v, w_g) is green, then both $\tau(v)$ and $\tau(w)$ have been modified according to the ratio on $\angle(w_g)$. Hence, the relationship $\tau(v) < \tau(w)$ is maintained. Finally, if (w_g, v) is blue then $\tau_2(v) \leq \tau_2(w_g) < \tau_2(w)$.

If $k \geq 1$ and (v_1, v) is blue, then we can apply the inductive hypothesis on both, (v, v_1) and the red edge (v_1, w) , and get $\tau_2(v) \leq \tau_2(v_1) < \tau_2(w)$. Finally, if $k > 1$ and (v, v_1) is green, then either $\sigma = v$ or $\tau(v)$ was set according to the ratio on $\angle(v_1)$, which implies especially that $\tau_2(v) \leq \tau_2((v_1)_r) = \tau_2(w)$ with equality if and only if $\tau_1(v) = \tau_1(w)$.

Case $y > \tau_1(\sigma)$: Note that, in this case, procedure ADJUST does not decrease τ for any vertex, that is, $\tau_2(v) \geq \tau_1(v)$ for every vertex v . We use the following order for the induction. An edge (v_1, w_1) is considered before an edge (v_2, w_2) if

⁴ With \leq , we abbreviate a case distinction between $=$ and $<$.

$v_2 < v_1$, or $v_1 = v_2 =: v$ and w_1 comes before w_2 in the counter-clockwise order around v starting from (v, v_g) .

Note that $y < \tau(X_r)$ and τ is always updated according to the ratio on the incident diagonal. Thus, by induction on the order in which the vertices are processed it follows immediately that $\tau_2(v) < \tau_2(X_r)$ for all vertices $v \neq X_r$. Hence, this is especially true if v is the last vertex according to $<$ before X_r .

Further, since τ did not decrease for any vertex, if (v, w) is an edge of $\text{DAG}_r(T)$ and $\tau(v)$ was not changed, then we have $\tau_2(v) = \tau_1(v) \leq \tau_1(w) \leq \tau_2(w)$. Assume now that $w \neq X_r$ and that $\tau(v)$ has changed.

If (v, w) is a green edge in $\text{DAG}_r(T)$, i.e., if $v = w_g$ then $\tau(w)$ is changed accordingly to the ratio on the diagonal of $\Delta(v)$. Thus, the relationship $\tau(v) \leq \tau(w)$ is maintained.

Consider now the case that (v, w) is an outgoing red edge of v or an incoming (in T) blue edge of v . Let $w = w_0, w_1, \dots, w_k = v_g$ be the neighbors of v in clockwise order from w to v_g —where $k = 1$ is possible. Observe that (w_i, v) , $i = 1, \dots, k - 1$, (if any) are blue. See Fig. 16. Observe further that for any $i = 1, \dots, k$ either (w_{i-1}, w_i) is a green edge or (w_i, w_{i-1}) is a red edge.

If $k = 1$ and $v = \sigma$ then $\tau_2(v) = y \leq \tau_1(w) \leq \tau_2(w)$, where $y = \tau_1(w)$ is only possible if (w, v) is blue and (v_g, w) is red. We distinguish four more cases: ($k = 1$ and $v \neq \sigma$) and $k > 1$ and for each of them whether the edge between w and w_1 is green or red. We start with $k = 1$: If (w, v_g) is red then $\tau_2(v) \leq \tau_2((v_g)_r) = \tau_2(w)$ with equality if and only if $\tau_1(v) = \tau_1((v_g)_r)$. If (w, v_g) is green then w and v are both neighbors on $\swarrow(v_g)$ and the relationship $\tau(v) < \tau(w)$ is maintained.

Consider now $k > 1$: Since $w_i, i = 1, \dots, k - 1$ is before w in the counter-clockwise ordering around v after v_g , we have by induction that $\tau_2(v) \leq \tau_2(w_1)$ with equality only if $\tau_1(v) = \tau_1(w_1)$ or $\langle v = \sigma, v_g, w_1 \rangle$ is a counter-clockwise cycle. If (w_1, w) is red, we observe that $v < w_1$ and we have again by induction that $\tau_2(w_1) < \tau_2(w)$.

If (w, w_1) is green then the relationship $\tau(w_1) \leq \tau(w)$ is maintained (even if $w = \sigma$, since τ does not decrease). It follows that $\tau_2(v) \leq \tau_2(w_1) \leq \tau_2(w)$. Observe that if $\langle v = \sigma, v_g, w_1 \rangle$ is a counter-clockwise cycle and $\tau_1(w_1) = \tau_1(w)$, then $\tau_2(v) = y < \tau_1(v_r) = \tau_1(w) = \tau_1(w_1) = \tau_2(w_1) = \tau_2(w)$ since moving σ to y respects the order along $\swarrow(\sigma_g)$ (condition (iii)). Thus, $\tau_2(v) = \tau_2(w)$ only if $\tau_1(v) = \tau_1(w)$.

Thus, in both cases, we have that Property DTL holds. This completes the proof that τ_2 is an ADT-labeling (condition (iii)).

$\swarrow_2(\sigma_g) = \swarrow_1(\sigma_g)$. Observe that all descendants of σ_g in $\text{DAG}_r(T)$ are on the blue path p_b or in the exterior of the cycle C' . Further, observe that the horizontal sides of the vertices in p_b can be constructed without knowing anything about the interior of C' . Thus $\swarrow(\sigma_g)$ does not change. Since $(\sigma_g)_r$ is also in the exterior of C' or on C' it follows that also the height of $\Delta(\sigma_g)$ remains unchanged. Thus $\swarrow(\sigma_g)$ is not changed.

$\langle R_1, R_2 \rangle$ is a linear morph. Case (i) in Lemma 4.2 is always fulfilled if the side is vertical or horizontal. Thus it suffices to consider the diagonal sides. The only vertex v for which the ratio $\lambda(v)$ changed was $v = \sigma$. However, since $\swarrow(\sigma_g)$ did not change it

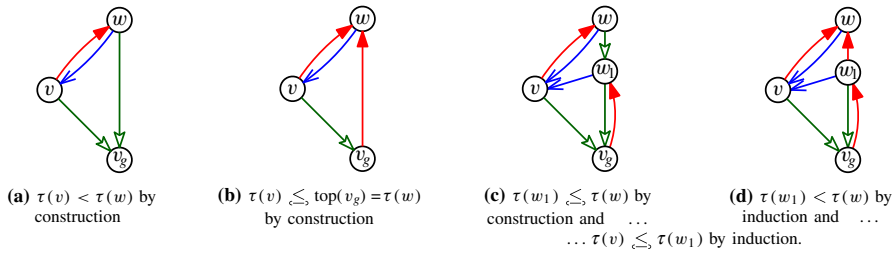


Fig. 16 Property DTL in the case $y > \tau(\sigma)$

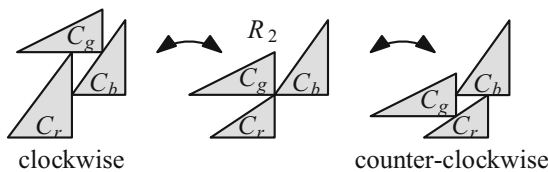
follows that $\angle_1(\sigma_g)$ and $\angle_2(\sigma_g)$ are parallel. Thus, Lemma 4.2 implies that $\langle R_1, R_2 \rangle$ is a linear morph. \square

5.2 A Flipping Algorithm

Recall that, given a Schnyder wood T and an oriented triangle C in T , the Schnyder wood T_C is obtained from T by flipping C . In the following theorem we show how to realize this flip geometrically with two linear morphs in the case in which C is a facial cycle.

Theorem 5.3 *Let R_1 be a non-degenerate RT-representation of a plane triangulation G corresponding to a Schnyder wood T . Let C be an oriented facial cycle in T . We can construct a sequence of two linear morphs $\langle R_1, R_2, R_3 \rangle$ such that R_3 is a non-degenerate RT-representation of G corresponding to a Schnyder wood T_C .*

Proof For the oriented facial cycle C , let C_r, C_g , and C_b be the vertices with outgoing red, green, and blue edge, respectively, in C . In order to flip C , we move C_g along the respective incident diagonal sides as sketched in the following figure.



More precisely, let τ_1 be the y-coordinates of the horizontal sides in R_1 . We first compute $\tau_2 \leftarrow \text{ADJUST}(\tau_1, T, C_g, \tau_1(C_b))$. If C is clockwise oriented, we then compute

$$\tau_3 \leftarrow \text{ADJUST}\left(\tau_2, T_C, C_g, \frac{\tau_2(C_g) + \max\{\tau_2(u) : u = C_r \text{ or } u_g = C_r\}}{2}\right).$$

If C is counter-clockwise oriented, we proceed as follows.

$$\tau_3 \leftarrow \text{ADJUST}\left(\tau_2, T_C, C_g, \frac{\tau_2(C_g) + \min\{\tau_2(u) : u = (C_b)_r \text{ or } u_g = C_b\}}{2}\right).$$

In each case the new y -coordinates y for C_g are chosen such that moving C_g to y respects the order along the respective incident diagonal. Thus, ADJUST can be applied. Also, τ_2 is an ADT-labeling of both, $\text{DAG}_r(T)$ and $\text{DAG}_r(T_C)$, and τ_3 is an ADT-labeling of $\text{DAG}_r(T_C)$. Let $R_2 = \text{RT}(T, \tau_2, R_o) = \text{RT}(T_C, \tau_2, R_o)$ and let $R_3 = \text{RT}(T_C, \tau_3, R_o)$. Since τ_2 and τ_3 are produced by ADJUST, by Lemma 5.2, both $\langle R_1, R_2 \rangle$ and $\langle R_2, R_3 \rangle$ are linear morphs. \square

5.3 Morphing Representations with the Same Schnyder Wood

In this section, we consider RT-representations corresponding to the same Schnyder wood.

Theorem 5.4 *Let R_1 and R_2 be two RT-representations of an n -vertex plane triangulation corresponding to the same Schnyder wood T . Then, there is a piecewise linear morph between R_1 and R_2 of length at most $2n$.*

The idea is to first transform the outer face to a canonical form, and then to move one vertex v per step to a new y -coordinate y such that the ratio $\lambda(v)$ is set to how it should be in R_2 . The order in which we process the vertices is such that ADJUST can be applied to the vertex v and the y -coordinate y . Recall that ADJUST does not alter the ratio λ , except for the currently processed vertex v .

Lemma 5.5 *Let $P = \{p_1 < \dots < p_n\}$ and $Q = \{q_1 < \dots < q_n\}$ be two sets of n reals each. If $P \neq Q$ then there is an $i \in \{1, \dots, n\}$ such that $p_i \neq q_i$ and P has no element between p_i and q_i .*

Proof We prove the lemma by induction on n . There is nothing to show if $n = 1$. If $n > 1$ and P and Q only differ in the last element p_n and q_n then let $i = n$. Otherwise, we apply the inductive hypothesis to $P \setminus \{p_n\}$ and $Q \setminus \{q_n\}$ which yields $p_i \neq q_i$, $i < n$, such that no element of $P \setminus \{p_n\}$ is between p_i and q_i . If p_n is not between p_i and q_i we are done. Otherwise we have $\dots < p_i < \dots < p_n < \dots < q_i < \dots < q_n$. Thus, $p_n \neq q_n$ and no element of P can be between p_n and q_n . \square

Corollary 5.6 *Let P and Q each be a set of n points on a segment s . We can move P to Q in n steps by moving one point per step and by maintaining the ordering of the points on s .*

Proof of Theorem 5.4 Let τ' be a topological ordering of the inner vertices of $\text{DAG}_r(T)$. We extend τ' to an ADT-labeling of $\text{DAG}_r(T)$ by setting $\tau'(X_b) = 0 = \tau'(X_g)$, and $\tau'(X_r) = n - 2$. With a sequence of at most n linear morphs we transform R_i , $i = 1, 2$, into an RT-representation $R' = \text{RT}(T, \tau', R_o)$, where R_o has the following canonical form: $\lrcorner(X_b) = \llcorner(X_g) = (0, 0)$, $\lrcorner(X_r) = \llcorner(X_r) = (0, n - 2)$, $\lrcorner(X_g) = \lrcorner(X_r) = (n - 2, n - 2)$, and each of $\lrcorner(X_r)$ and $\lrcorner(X_b)$ has length one. In the first morph, we cut the extruding parts of the outer triangles. In the second morph, we independently scale the x - and y -coordinates of the corners and translate the drawing, to fit the corners as indicated. In the third step, we adjust the lengths of $\lrcorner(X_r)$ and $\lrcorner(X_b)$. In the first morph the slope of no side is changed, in the second

morph no ratio is changed, and in the third morph there are only four sides that are changed, which are not incident to any other triangle. Thus, by Lemma 4.2, the three morphs are linear. Let the resulting RT-representation be R'_i .

We now process the vertices in a reversed topological ordering on $\text{DAG}_b(T)$. This will ensure that once a vertex has been processed, it will not be modified by ADJUST anymore; this is because the vertices modified by ADJUST are determined by the red and green edges, which are both reversed in $\text{DAG}_b(T)$. We process a vertex w as follows. Let τ be the function describing the current y -coordinates of the horizontal sides. Let $\mathcal{G}(w) = \{v \in V : w = v_g\}$ and let $P = \{\tau(v) : v \in \mathcal{G}(w)\}$. For $v \in \mathcal{G}(w)$, let $y(v)$ be such that

$$\frac{y(v) - \tau(w)}{\tau(w_r) - \tau(w)} = \frac{\tau'(v) - \tau'(w)}{\tau'(w_r) - \tau'(w)},$$

i.e., placing $\triangleleft(v)$, $v \in \mathcal{G}(w)$, on the y -coordinate $y(v)$ cuts $\nearrow(w)$ with the same ratio as in R' . Let $Q = \{y(v) : v \in \mathcal{G}(w)\}$. By Corollary 5.6, we can order $\mathcal{G}(w) = \{v_1, \dots, v_k\}$ such that replacing in the i th step $\tau(v_i)$ by $y(v_i)$ maintains the ordering of $\{\tau(v) : v \in \mathcal{G}(w)\}$. Since τ' is a topological ordering, we will not move $\perp(v_i)$ to an end vertex of $\nearrow(w)$. For $i = 1, \dots, k$ we now call $\tau \leftarrow \text{ADJUST}(\tau, T, v_i, y(v_i))$. By Lemma 5.2, each such call yields a single linear morph.

After processing all vertices w in a reversed topological ordering of $\text{DAG}_b(T)$ and all vertices in $\mathcal{G}(w)$ in the order given above, we have obtained an RT-representation R in which any right corner cuts its incident diagonal with the same ratio as in R' . Since the outer face is fixed, this implies that $R = R'$. Observe that $\mathcal{G}(w)$, $w \in V$, is a partition of the set of inner vertices. Hence, we get at most one morphing step for each of the $n - 3$ inner vertices. This ends the proof. \square

Combining the results of Sects. 5.1, 5.2, and 5.3 yields the main result of the section.

Proof of Theorem 5.1 First, we transform R_1 into a non-degenerate RT-representation R with Schnyder wood T_1 and a canonical form of the outer face in $\mathcal{O}(n)$ linear morphing steps, by Theorem 5.4. Then, we perform the ℓ facial flips. As described in Theorem 5.3, we can do so using two linear morphs for each flip. This yields an RT-representation R' with Schnyder wood T_2 . Finally, we transform R' into R_2 in $\mathcal{O}(n)$ linear morphing steps, by Theorem 5.4. This yields a total of $\mathcal{O}(n + \ell)$ linear morphs. Each linear morph can be computed by one application of ADJUST, which runs in linear time. \square

6 Finding a Sequence of Facial Flips

It follows from Theorems 3.4 and 5.1 that there is a piecewise linear morph between two RT-representations of a plane triangulation if and only if the respective Schnyder woods can be obtained from each other by flipping internal faces only. Note that this condition is always satisfied if the triangulation is 4-connected and the topmost vertex is the same in both RT-representations. On the other hand, if the graph contains separating triangles, we have to decide whether there is such a sequence of facial

flips. We will show in Lemma 6.3 that this can be decided efficiently and that, in the positive case, there exists a sequence whose length is at most quadratic in the number of vertices. In the proof of Lemma 6.4, we then show how such a sequence of facial flips can also be computed in quadratic time. With the run time from Theorem 5.1, this establishes our final result.

Theorem 6.1 *Let R_1 and R_2 be two RT-representations of an n -vertex plane triangulation. We can decide in $\mathcal{O}(n^2)$ time whether there is a morph between R_1 and R_2 and, if so, a piecewise linear morph with $\mathcal{O}(n^2)$ linear morphing steps can be computed in $\mathcal{O}(n^3)$ time.*

Corollary 6.2 *There is a piecewise linear morph with $\mathcal{O}(n^2)$ linear morphing steps between two RT-representations of a 4-connected plane triangulation if and only if the topmost vertex is the same in both RT-representations.*

Since there is a one-to-one correspondence between Schnyder woods of a plane triangulation and its 3-orientations, we will omit the colors in the following. A careful reading of Brehm [17] and Felsner [29] reveals the subsequent properties of 3-orientations. The set of 3-orientations of a triangulation forms a distributive lattice with respect to the following ordering. $T_1 \leq T_2$ if and only if T_1 can be obtained from T_2 by a sequence of flips on some counter-clockwise triangles. The minimum element is the unique 3-orientation without counter-clockwise cycles. Moreover, given a 3-orientation T and a triangle t , the number of occurrences of t in any flip-sequence between T and the minimum 3-orientation is the same—provided that the flip sequence contains only counter-clockwise triangles. Let this number be the potential $\pi_T(t)$. See Fig. 17 for an example.

Observe that π_T is distinct for distinct T . Moreover, given a triangle t , the potential of the meet $T_1 \wedge T_2$ (i.e., the infimum) of two 3-orientations T_1 and T_2 is $\min(\pi_{T_1}(t), \pi_{T_2}(t))$ while the potential of the join $T_1 \vee T_2$ (i.e., the supremum) of T_1 and T_2 is $\max(\pi_{T_1}(t), \pi_{T_2}(t))$. The potential π_T can be computed in quadratic time for a fixed 3-orientation T of an n -vertex triangulation: At most $\mathcal{O}(n^2)$ flips have to be performed in order to reach the minimum 3-orientation. With a linear-time preprocessing, we can store all initial counter-clockwise triangles in a list. After each flip, the list can be updated in constant time.

Lemma 6.3 *Let T_1 and T_2 be two 3-orientations of an n -vertex triangulation. T_1 can be obtained from T_2 by a sequence of facial flips if and only if $\pi_{T_1}(t) - \pi_{T_2}(t) = 0$ for all separating triangles t . Moreover, if T_1 can be obtained from T_2 by a sequence of facial flips, then any sequence of counter-clockwise flips between T_1 and the meet $T_1 \wedge T_2$ followed by any sequence of clockwise flips to T_2 consists of $\mathcal{O}(n^2)$ facial flips.*

Proof Observe that going from T_1 to the meet $T_1 \wedge T_2$ involves

$$\pi_{T_1}(t) - \min(\pi_{T_1}(t), \pi_{T_2}(t)) \in \{0, \pi_{T_1}(t) - \pi_{T_2}(t)\}$$

counter-clockwise flips on triangle t , and going from the meet $T_1 \wedge T_2$ to T_2 involves

$$\pi_{T_2}(t) - \min(\pi_{T_1}(t), \pi_{T_2}(t)) \in \{0, \pi_{T_2}(t) - \pi_{T_1}(t)\}$$

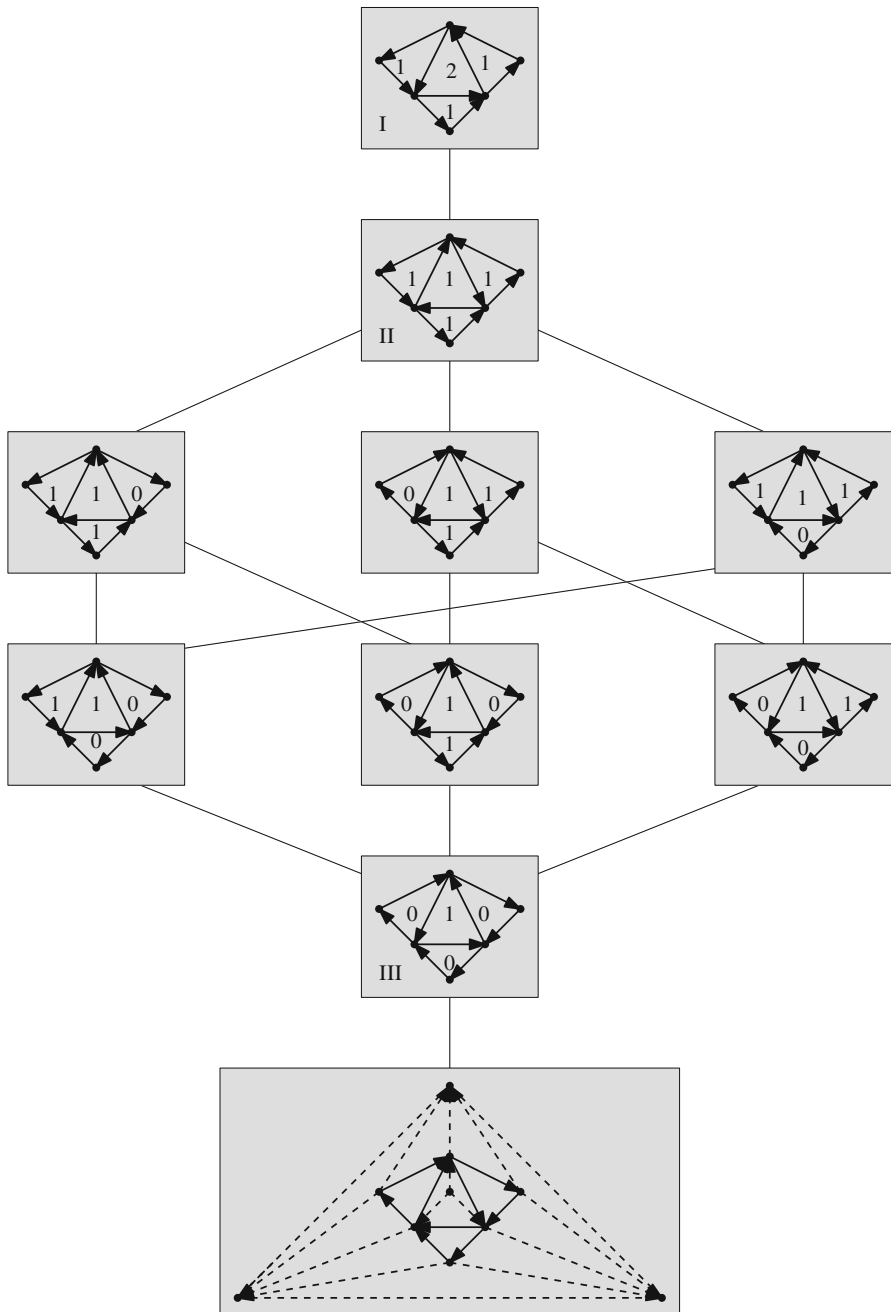


Fig. 17 The lattice of all 3-orientations of a graph. The whole graph is only drawn in the minimum 3-orientation. The dashed edges are not repeated in the other drawings—they do not change their direction. Face labels indicate potentials. Observe that the inner solid face is actually a separating triangle (there are not-drawn dashed edges inside)

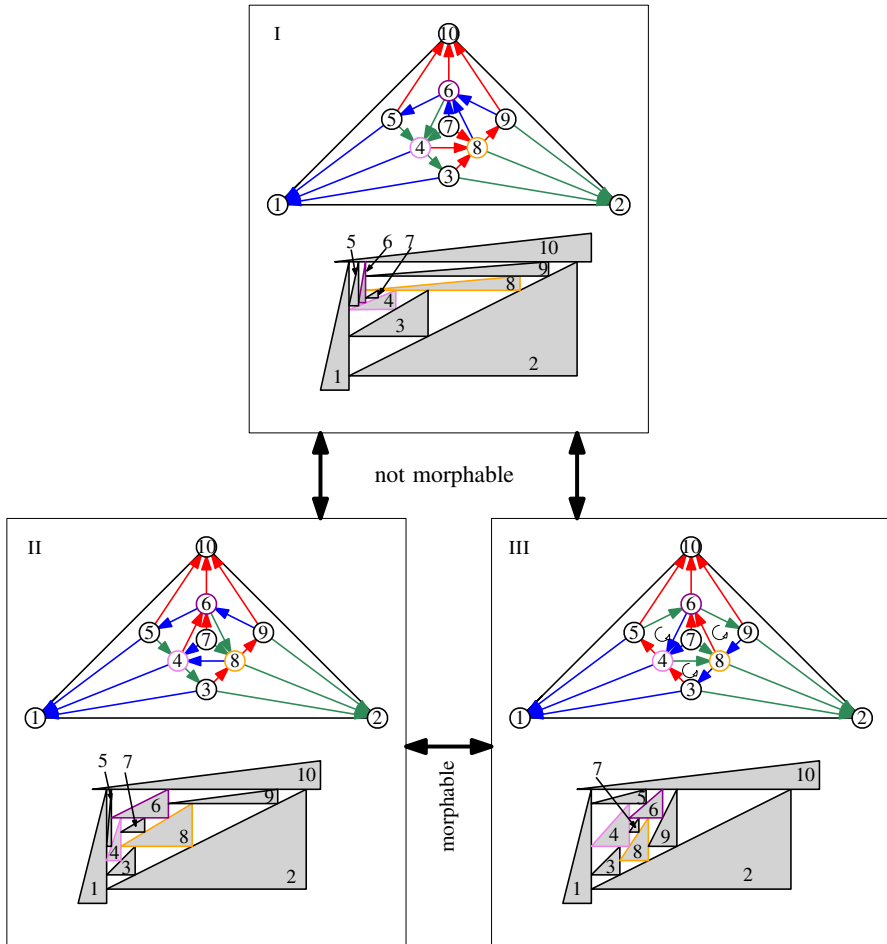


Fig. 18 RT-representations corresponding to orientations I, II, and III of Fig. 17, which are not morphable one into the other

clockwise flips on triangle t . Thus, if $\pi_{T_1}(t) - \pi_{T_2}(t) = 0$ for all separating triangles t , then no flip must be performed on a separating triangle. Then, the total number of flips is bounded by $\sum_{t \text{ face}} (\pi_{T_1}(t) + \pi_{T_2}(t)) \in \mathcal{O}(n^2)$.

Assume now that there is a sequence $T_1 = T'_0, T'_1, \dots, T'_\ell, T'_{\ell+1} = T_2$ of 3-orientations such that $T'_{i+1}, i = 0, \dots, \ell$, is obtained from T'_i by a (clockwise or counter-clockwise) facial flip. We show by induction on ℓ that $\pi_{T_1}(t) - \pi_{T_2}(t) = 0$ for all separating triangles t . If $\ell = 0$, let t_0 be the triangle that has to be flipped in order to go from T_1 to T_2 . Then, t_0 is a face and $\pi_{T_1}(t) - \pi_{T_2}(t) = 0$ for $t \neq t_0$. Assume now that $\ell \geq 1$. Let t be a separating triangle. Then

$$\pi_{T_1}(t) - \pi_{T_2}(t) = \underbrace{\pi_{T_1}(t) - \pi_{T'_\ell}(t)}_{=0 \text{ by IH}} + \underbrace{\pi_{T'_\ell}(t) - \pi_{T_2}(t)}_{=0 \text{ by IH}} = 0.$$

□

While a sequence of counter-clockwise flips from a 3-orientation T_1 to the minimum of the lattice can always be found by iteratively flipping any counter-clockwise triangle, this is no longer true if we want to find a path from T_1 to the meet $T_1 \wedge T_2$ of two 3-orientations T_1 and T_2 . Here we have to follow the potential difference:

Lemma 6.4 *Let T_1 and T_2 be two 3-orientations of an n -vertex triangulation. If T_2 can be obtained from T_1 by a sequence of facial flips then such a sequence can be computed in $\mathcal{O}(n^2)$ time.*

Proof We construct the sequence of facial flips as follows: Starting with T_1 we first find a sequence of flips down to the meet and then up again to T_2 . By the proof of Lemma 6.3, this sequence consists of facial flips only. Since $\pi_{T_1 \wedge T_2}(t) = \min(\pi_{T_1}(t), \pi_{T_2}(t))$ for all facial triangles and since distinct 3-orientations have distinct potentials, such a path can be found as follows.

Let $T = T_1$. While $\pi_T(t) > \pi_{T_2}(t)$ for some counter-clockwise facial cycle t , pick such a cycle and flip it. Now $T = T_1 \wedge T_2$. While $\pi_T(t) < \pi_{T_2}(t)$ for some clockwise facial cycle t , pick such a cycle and flip it.

At most $\mathcal{O}(n^2)$ flips have to be performed to reach the meet. In the first while-loop, we only store the counter-clockwise facial cycles with $\pi_T(t) > \pi_{T_2}(t)$ in a list and in the second while-loop the clockwise facial cycles with $\pi_T(t) < \pi_{T_2}(t)$. This list can still be updated in constant time after each flip. \square

Observe that there might be a piecewise linear morph between two RT-representations even though a separating triangle in the respective Schnyder woods is oriented in opposite directions. E.g., consider the 3-orientations II and III of the graph in Figs. 17 and 18. Moreover, there might be two RT-representations such that any separating triangle is oriented in the same way in the two respective Schnyder woods, however, there is no piecewise linear morph between the two representations. E.g., consider the 3-orientations III and I of the graph in Figs. 17 and 18, every path in the lattice between them passes through a 3-orientation in which the unique separating triangle is flipped.

7 Conclusions and Open Problems

In this paper, we initiated the study of morphs between contact representations of graphs. In particular, we have studied morphs between RT-representations of plane triangulations. We have shown that if such a morph exists, then there is a piecewise linear morph of length $\mathcal{O}(n^2)$. It would be interesting to explore lower bounds on the length of a piecewise linear morph. Observe that the worst-case minimum length of a flip sequence containing only facial cycles does not have to be a lower bound for the length of a piecewise linear morph, since some flips could be parallelized. Additionally, bounds on the resolution throughout our morphs would be worth investigating; however, it is unclear whether the “ratio fixing” we use in the procedure ADJUST would allow nice bounds. A major open direction is whether our results can be lifted to general plane graphs, e.g., through the use of compatible triangulations [11, 51]. Note that such compatible triangulations would need to be formed while preserving the

conditions for the existence of a morph, i.e., without introducing the need to flip a separating triangle.

Finally, beyond the context of RT-representations, many other families of geometric objects could be considered. For example, morphing degenerate contact representations of line segments generalizes planar morphing, by treating contact points as vertices.

Acknowledgements We thank Stefan Felsner, Niklas Heinsohn, and Anna Lubiw for interesting discussions on this subject.

Funding Open Access funding enabled and organized by Projekt DEAL.

Data Availability Data sharing is not applicable to this article as no datasets were generated or analysed during the current study.

Open Access This article is licensed under a Creative Commons Attribution 4.0 International License, which permits use, sharing, adaptation, distribution and reproduction in any medium or format, as long as you give appropriate credit to the original author(s) and the source, provide a link to the Creative Commons licence, and indicate if changes were made. The images or other third party material in this article are included in the article's Creative Commons licence, unless indicated otherwise in a credit line to the material. If material is not included in the article's Creative Commons licence and your intended use is not permitted by statutory regulation or exceeds the permitted use, you will need to obtain permission directly from the copyright holder. To view a copy of this licence, visit <http://creativecommons.org/licenses/by/4.0/>.

References

1. Alamdari, S., Angelini, P., Barrera-Cruz, F., Chan, T.M., Da Lozzo, G., Di Battista, G., Frati, F., Haxell, P., Lubiw, A., Patrignani, M., Roselli, V., Singla, S., Wilkinson, B.T.: How to morph planar graph drawings. *SIAM J. Comput.* **46**(2), 824–852 (2017)
2. Alamdari, S., Angelini, P., Chan, T.M., Di Battista, G., Frati, F., Lubiw, A., Patrignani, M., Roselli, V., Singla, S., Wilkinson, B.T.: Morphing planar graph drawings with a polynomial number of steps. In: 24th Annual ACM-SIAM Symposium on Discrete Algorithms (New Orleans 2013), pp. 1656–1667. SIAM, Philadelphia (2012)
3. Alt, H., Guibas, L.J.: Discrete geometric shapes: matching, interpolation, and approximation. In: *Handbook of Computational Geometry*, pp. 121–153. North-Holland, Amsterdam (2000)
4. Andreev, E.M.: Convex polyhedra in Lobachevskii spaces. *Sbornik Math.* **10**(3), 413–440 (1970)
5. Angelini, P.: Monotone drawings of graphs with few directions. *Inform. Process. Lett.* **120**, 16–22 (2017)
6. Angelini, P., Bekos, M.A., Montecchiani, F., Pfister, M.: On morphs of 1-plane graphs. *J. Comput. Geom.* **13**(1), 244–262 (2022)
7. Angelini, P., Da Lozzo, G., Di Battista, G., Frati, F., Patrignani, M., Roselli, V.: Morphing planar graph drawings optimally. In: 41st International Colloquium on Automata, Languages, and Programming (Copenhagen 2014). Part I. *Lecture Notes in Comput. Sci.*, vol. 8572, pp. 126–137. Springer, Heidelberg (2014)
8. Angelini, P., Da Lozzo, G., Frati, F., Lubiw, A., Patrignani, M., Roselli, V.: Optimal morphs of convex drawings. In: 31st International Symposium on Computational Geometry (Eindhoven 2015). *Leibniz Int. Proc. Inform.*, vol. 34, pp. 126–140. Leibniz-Zent. Inform., Wadern (2015)
9. Angelini, P., Frati, F., Patrignani, M., Roselli, V.: Morphing planar graph drawings efficiently. In: 21st International Symposium on Graph Drawing (Bordeaux 2013). *Lecture Notes in Comput. Sci.*, vol. 8242, pp. 49–60. Springer, Cham (2013)
10. Arnold, D.N., Rogness, J.: Möbius transformations revealed. *Not. Am. Math. Soc.* **55**(10), 1226–1231 (2008)
11. Aronov, B., Seidel, R., Souvaine, D.: On compatible triangulations of simple polygons. *Comput. Geom.* **3**(1), 27–35 (1993)

12. Arseneva, E., Bose, P., Cano, P., D'Angelo, A., Dujmović, V., Frati, F., Langerman, S., Tappini, A.: Pole dancing: 3D morphs for tree drawings. *J. Graph Algorithms Appl.* **23**(3), 579–602 (2019)
13. Barrera-Cruz, F., Borrizzo, M., Da Lozzo, G., Di Battista, G., Frati, F., Patrignani, M., Roselli, V.: How to morph a tree on a small grid. In: 16th International Algorithms and Data Structures Symposium (Edmonton 2019). *Lecture Notes in Comput. Sci.*, vol. 11646, pp. 57–70. Springer, Cham (2019)
14. Barrera-Cruz, F., Haxell, P., Lubiw, A.: Morphing Schnyder drawings of planar triangulations. *Discrete Comput. Geom.* **61**(1), 161–184 (2019)
15. Biedl, Th., Lubiw, A., Petrick, M., Spriggs, M.: Morphing orthogonal planar graph drawings. *ACM Trans. Algorithms* **9**(4), # 29 (2013)
16. Bowen, C., Durocher, S., Löffler, M., Rounds, A., Schulz, A., Tóth, Cs.D.: Realization of simply connected polygonal linkages and recognition of unit disk contact trees. In: 23rd International Symposium on Graph Drawing and Network Visualization (Los Angeles 2015). *Lecture Notes in Comput. Sci.*, vol. 9411, pp. 447–459. Springer, Cham (2015)
17. Brehm, E.: 3-Orientations and Schnyder 3-Tree-Decompositions. MSc thesis, Freie Universität Berlin (2000). <https://page.math.tu-berlin.de/~felsner/Diplomarbeiten/brehm.ps.gz>
18. Brightwell, G.R., Scheinerman, E.R.: Representations of planar graphs. *SIAM J. Discrete Math.* **6**(2), 214–229 (1993)
19. Cairns, S.S.: Deformations of plane rectilinear complexes. *Am. Math. Mon.* **51**(5), 247–252 (1944)
20. Chambers, E.W., Erickson, J., Lin, P., Parsa, S.: How to morph graphs on the torus. In: 2021 ACM-SIAM Symposium on Discrete Algorithms, pp. 2759–2778. SIAM, Philadelphia (2021)
21. Chaplick, S., Kindermann, Ph., Klawitter, J., Rutter, I., Wolff, A.: Morphing rectangular duals (2021). [arXiv:2112.03040](https://arxiv.org/abs/2112.03040)
22. Chaplick, S., Kobourov, S.G., Ueckerdt, T.: Equilateral L-contact graphs. In: 39th International Workshop on Graph-Theoretic Concepts in Computer Science (Lübeck 2013). *Lecture Notes in Comput. Sci.*, vol. 8165, pp. 139–151. Springer, Heidelberg (2013)
23. Connelly, R., Demaine, E.D., Demaine, M.L., Fekete, S.P., Langerman, S., Mitchell, J.S.B., Ribó, A., Rote, G.: Locked and unlocked chains of planar shapes. *Discrete Comput. Geom.* **44**(2), 439–462 (2010)
24. Da Lozzo, G., Devanny, W.E., Eppstein, D., Johnson, T.: Square-contact representations of partial 2-trees and triconnected simply-nested graphs. In: 28th International Symposium on Algorithms and Computation (Phuket 2017). *Leibniz Int. Proc. Inform.*, vol. 92, # 24. Leibniz-Zent. Inform., Wadern (2017)
25. Da Lozzo, G., Di Battista, G., Frati, F., Patrignani, M., Roselli, V.: Upward planar morphs. *Algorithmica* **82**(10), 2985–3017 (2020)
26. Demaine, E.D., O'Rourke, J.: *Geometric Folding Algorithms: Linkages*. Cambridge University Press, Cambridge, Origami. Polyhedra (2007)
27. Di Giacomo, E., Liotta, G., Mchedlidze, T.: Lower and upper bounds for long induced paths in 3-connected planar graphs. *Theoret. Comput. Sci.* **636**, 47–55 (2016)
28. Erickson, J., Lin, P.: Planar and toroidal morphs made easier. In: 29th International Symposium on Graph Drawing and Network Visualization (Tübingen 2021). *Lecture Notes in Comput. Sci.*, vol. 12868, pp. 123–137. Springer, Cham (2021)
29. Felsner, S.: Lattice structures from planar graphs. *Electron. J. Comb.* **11**(1), # R15 (2004)
30. Felsner, S., Francis, M.C.: Contact representations of planar graphs with cubes. In: 27th Annual Symposium on Computational Geometry (Paris 2011), pp. 315–320. ACM, New York (2011)
31. Felsner, S., Rote, G.: On primal-dual circle representations. In: 2nd Symposium on Simplicity in Algorithms (San Diego 2019). *OASiCS OpenAccess Ser. Inform.*, vol. 69, # 8. Leibniz-Zent. Inform., Wadern (2019)
32. Felsner, S., Schrezenmaier, H., Steiner, R.: Equiangular polygon contact representations. In: 44th International Workshop on Graph-Theoretic Concepts in Computer Science (Cottbus 2018). *Lecture Notes in Comput. Sci.*, vol. 11159, pp. 203–215. Springer, Cham (2018)
33. Floater, M.S., Gotsman, C.: How to morph tilings injectively. *J. Comput. Appl. Math.* **101**(1–2), 117–129 (1999)
34. de Fraysseix, H., Ossona de Mendez, P.: Representations by contact and intersection of segments. *Algorithmica* **47**(4), 453–463 (2007)
35. de Fraysseix, H., Ossona de Mendez, P., Rosenstiehl, P.: On triangle contact graphs. *Comb. Probab. Comput.* **3**(2), 233–246 (1994)

36. van Goethem, A., Verbeek, K.: Optimal morphs of planar orthogonal drawings. In: 34th International Symposium on Computational Geometry (Budapest 2018). Leibniz Int. Proc. Inform., vol. 99, # 42. Leibniz-Zent. Inform., Wadern (2018)
37. van Goethem, A., Speckmann, B., Verbeek, K.: Optimal morphs of planar orthogonal drawings II. In: 27th International Symposium on Graph Drawing and Network Visualization (Prague 2019). Lecture Notes in Comput. Sci., vol. 11904, pp. 33–45. Springer, Cham (2019)
38. Gonçalves, D., Lévêque, B., Pinlou, A.: Triangle contact representations and duality. *Discrete Comput. Geom.* **48**(1), 239–254 (2012)
39. Gotsman, C., Surazhsky, V.: Guaranteed intersection-free polygon morphing. *Comput. Graph.* **25**(1), 67–75 (2001)
40. Kleist, L., Klemz, B., Lubiw, A., Schlipf, L., Staals, F., Strash, D.: Convexity-increasing morphs of planar graphs. *Comput. Geom.* **84**, 69–88 (2019)
41. Klemz, B.: Convex drawings of hierarchical graphs in linear time, with applications to planar graph morphing. In: 29th Annual European Symposium on Algorithms. Leibniz Int. Proc. Inform., vol. 204, # 57. Leibniz-Zent. Inform., Wadern (2021)
42. Kobourov, S.G., Landis, M.: Morphing planar graphs in spherical space. *J. Graph Algorithms Appl.* **12**(1), 113–127 (2008)
43. Kobourov, S., Ueckerdt, T., Verbeek, K.: Combinatorial and geometric properties of planar Laman graphs. In: 24th Annual ACM-SIAM Symposium on Discrete Algorithms (New Orleans 2013), pp. 1668–1678. SIAM, Philadelphia (2013)
44. Koebe, P.: Kontaktprobleme der konformen Abbildung. *Ber. Sächs. Akad. Wiss. Leipzig Math. Phys. Kl.* **88**, 141–164 (1936)
45. Laman, G.: On graphs and rigidity of plane skeletal structures. *J. Eng. Math.* **4**(4), 331–340 (1970)
46. Nöllenburg, M., Prutkin, R., Rutter, I.: On self-approaching and increasing-chord drawings of 3-connected planar graphs. *J. Comput. Geom.* **7**(1), 47–69 (2016)
47. Schnyder, W.: Embedding planar graphs on the grid. In: 1st Annual ACM-SIAM Symposium on Discrete Algorithms (San Francisco 1990), pp. 138–148. SIAM, Philadelphia (1990)
48. Schramm, O.: Combinatorially Prescribed Packings and Applications to Conformal and Quasiconformal Maps. PhD thesis, Princeton University (1990)
49. Schrezenmaier, H.: Homothetic triangle contact representations. In: 43rd International Workshop on Graph-Theoretic Concepts in Computer Science (Eindhoven 2017). Lecture Notes in Comput. Sci., vol. 10520, pp. 425–437. Springer, Cham (2017)
50. Surazhsky, V., Gotsman, C.: Controllable morphing of compatible planar triangulations. *ACM Trans. Graph.* **20**(4), 203–231 (2001)
51. Thomassen, C.: Deformations of plane graphs. *J. Comb. Theory Ser. B* **34**(3), 244–257 (1983)
52. Thomassen, C.: Interval representations of planar graphs. *J. Comb. Theory Ser. B* **40**(1), 9–20 (1986)
53. Tutte, W.T.: How to draw a graph. *Proc. Lond. Math. Soc.* **13**, 743–767 (1963)

Publisher's Note Springer Nature remains neutral with regard to jurisdictional claims in published maps and institutional affiliations.

Authors and Affiliations

Patrizio Angelini¹  · Steven Chaplick²  · Sabine Cornelsen³  ·
Giordano Da Lozzo⁴  · Vincenzo Roselli⁴ 

Patrizio Angelini
pangelini@johncabot.edu

Steven Chaplick
s.chaplick@maastrichtuniversity.nl

Sabine Cornelsen
sabine.cornelsen@uni-konstanz.de

Giordano Da Lozzo
giordano.dalozzo@uniroma3.it

Vincenzo Roselli
vincenzo.roselli@uniroma3.it

- ¹ John Cabot University, Rome, Italy
- ² Maastricht University, Maastricht, The Netherlands
- ³ University of Konstanz, Konstanz, Germany
- ⁴ Roma Tre University, Rome, Italy